

Copyright
by
Tanzeen Yusuff
2014

**The Dissertation Committee for Tanzeen Yusuff Certifies that this is the
approved version of the following dissertation:**

**CHARACTERIZATION OF CODON OPTIMIZED WILD TYPE TDP-43
MEDIATED NEURODEGENERATION IN A *DROSOPHILA* MODEL FOR ALS**

Committee:

George R. Jackson, MD, PhD, Supervisor,
Chair

Volker Neugebauer, MD, PhD

Kelly T. Dineley, PhD

Neslihan M. Martinez, PhD

Yogesh Wairkar, PhD

Brian C. Kraemer, PhD

Dean, Graduate School

**CHARACTERIZATION OF CODON OPTIMIZED WILD TYPE TDP-43
MEDIATED NEURODEGENERATION IN A *DROSOPHILA* MODEL FOR ALS**

by

Tanzeen Yusuff, B.S.

Dissertation

Presented to the Faculty of the Graduate School of
The University of Texas Medical Branch
in Partial Fulfillment
of the Requirements
for the Degree of

Doctor of Philosophy

The University of Texas Medical Branch

May, 2014

Dedication

To my parents, for their endless support and encouragement.

Acknowledgements

I would like to thank my mentor Dr. George R. Jackson for his mentorship during my years of graduate school at UTMB. I am thankful to have had the opportunity to learn a great deal from him. His enthusiasm for teaching, particularly fly genetics, has only strengthened and encouraged my experience as a graduate student. His continued support and patience has been a tremendous help over the last few years. I sincerely appreciate and thank him for all the time and effort he has invested in guiding me through the projects in his lab.

I would also like to thank all of the members of my dissertation committee: Dr. Volker Neugebauer, Dr. Kelly T. Dineley, Dr. Neslihan M. Martinez, Dr. Yogesh Wairkar and Dr. Brian C. Kraemer from University of Washington. Their continued support and constructive feedback have been very helpful. I would like to thank Dr. Robin Hiesinger from University of Texas Southwestern for allowing me the opportunity to visit his lab and perform the ERG experiments. I would also like to thank his research assistant Daniel Epstein, who took the time to teach me the ERG techniques and to help me with the experiments and analysis. I would like to thank Dr. Fen-Biao Gao from University of Massachusetts for kindly providing the human TDP-43 transgenic flies and Dr. Hugo J. Bellen from Baylor College of Medicine for kindly providing the *equate*-GAL4 flies.

I would like to thank all the past members of the Jackson lab. I have had the opportunity to learn a great deal from Dr. Shreyasi Chatterjee, Dr. Suren Ambegaokar, Dr. Bidisha Roy and Mathieu Bakhoun. They have always been very generous with all of their help and have patiently taught me various

laboratory techniques that I have used for this project. I truly appreciate all the time they have invested in helping me throughout my graduate school years. I also want to thank my other fellow graduate students from Jackson lab, Darshana Choksi and Amy Hill, for their kindness and friendship. I want to thank Dr. Rakez Kaye for his support and encouragement throughout the years, Dr. Adriana Paulucci for her help with the confocal microscopy, Dr. Fernanda Laezza, whom I have had the opportunity to learn from during my rotation in her lab. I want to thank the current Neuroscience Graduate Program director, Dr. Giulio Taglialetela, the past director, Dr. Volker Neugebauer, and the Pharmacology and Toxicology Graduate Program director, Dr. Kenneth M. Johnson for their helpful guidance over the years.

Lastly, I want to thank my family, especially my parents. Their unconditional love, patience and encouragement have been an integral part of my graduate school career.

**CHARACTERIZATION OF CODON OPTIMIZED WILD TYPE TDP-43
MEDIATED NEURODEGENERATION IN A *DROSOPHILA* MODEL FOR ALS**

Publication No. _____

Tanzeen Yusuff, Ph.D.

The University of Texas Medical Branch, 2014

Supervisor: George R. Jackson

ABSTRACT

TAR DNA Binding Protein-43 (TDP-43) is known to mediate neurodegeneration associated with amyotrophic lateral sclerosis (ALS) and frontotemporal lobar degeneration-ubiquitin (FTLD-U). The exact mechanism by which TDP-43 exerts toxicity in patient brains remains unclear. In a *Drosophila* model, we have identified robust gain of function phenotypes produced by misexpression of insect codon optimized wild type TDP-43 using the binary GAL4/UAS system, as well as direct promoter fusion constructs with glass promoter. Codon optimized TDP-43 misexpression causes robust phenotypes in the adult eye, wings and bristles in the notum. Compared to human transgenic flies, the codon optimized flies express more protein that forms higher molecular weight species. Both nuclear and cytoplasmic expression of TDP-43 were detected along with cytoplasmic aggregation. Further characterization of the adult retina shows a disruption of the morphology and function of the photoreceptor neurons along with acidic vacuoles that are positive for autophagy markers. Moreover, changes in the protein levels of mTOR signaling pathway

substrate were detected upon TDP-43 misexpression. Based on this observation, we believe that TDP-43 has the propensity to form toxic protein aggregates when too much protein is present via a gain-of-function mechanism. Such toxic overload leads to an increase in cellular protein degradation pathways like autophagy. The robust phenotypes seen with TDP-43 misexpression are ideal for genetic screens to identify new modifiers and therapeutic targets. The codon optimized TDP-43 model is a novel and improved model in *Drosophila* that can be used to better understand the exact disease mechanism of TDP-43 proteinopathies.

TABLE OF CONTENTS

List of Tables	x
List of Figures	xi
CHAPTER I: TDP-43 MEDIATED NEURODEGENERATION	1
1.1 TDP-43 Proteinopathies	1
Amyotrophic lateral sclerosis	1
Frontotemporal lobar degeneration	2
Diagnosis and current treatments	3
TDP-43 protein at a glance	4
TDP-43 in neurodegeneration	5
1.2 Animal Models for TDP-43 Proteinopathies	6
1.3 <i>Drosophila</i> Models for Neurodegeneration	8
<i>Drosophila</i> eye as a model	9
Neurodegeneration in flies	11
CHAPTER II: MATERIALS AND METHODS	16
2.1 Fly Stocks and Genetics	16
Codon optimized TDP-43 flies	16
Genotypes	17
2.2 Immunohistochemistry	18
2.3 Immunoblotting	20
2.4 LysoTracker Staining	21
2.5 Electroretinogram	22
2.6 Optical Neutralization and Pseudopupil	23
2.7 Microscopy	23
2.8 Quantification and Statistical Analysis	25
CHAPTER III: ROBUST PHENOTYPES OF THE CODON OPTIMIZED TDP-43 <i>DROSOPHILA</i> MODEL	29
3.1 Introduction	29
Current <i>Drosophila</i> models for TDP-43 proteinopathies	29
<i>Drosophila</i> model with codon optimized TDP-43	31

3.2 Results	33
Codon optimized TDP-43 misexpression in the <i>Drosophila</i> eye causes robust phenotypes	33
Codon optimized TDP-43 misexpression in wings causes inflation defects and loss of bristles	35
Misexpression of codon optimized TDP-43 mimics cellular and molecular phenotypes seen in pathological disease state....	36
3.3 Conclusions	38
CHAPTER IV: MISEXPRESSION OF TDP-43 AND AUTOPHAGY	52
3.1 Introduction	52
Autophagy in neurodegeneration	52
Autophagy signaling and machinery	53
Autophagy in TDP-43 proteinopathies	55
3.2 Results	56
Morphological and functional disruption of the photoreceptor neurons upon TDP-43 misexpression	56
TDP-43 misexpression induced vacuoles are similar to autophagic intermediates	58
TDP-43 misexpression changes the levels of proteins involved in mTOR signaling	60
3.3 Conclusions	62
CHAPTER V: SUMMARY AND FUTURE DIRECTIONS	72
5.1 Relevance of Codon Optimized Disease Model for TDP-43 Proteinopathies	72
Non-cell-autonomous toxicity in codon optimized TDP-43 transgenic model	72
Codon optimized TDP-43 transgenic model and genetic screens	73
5.2 Autophagy and TDP-43	74
5.3 Concluding Remarks	76
Bibliography	77
Vita	96

List of Tables

Table 3.1: Summary of TDP-43 misexpression in the fly eye	51
---	----

List of Figures

Figure 1.1: Schematic of the TDP-43 protein.....	14
Figure 1.2: The GAL4-UAS binary system	15
Figure 2.1: pExpress UAS/glass vector	27
Figure 2.2: Schematic of larval eye disc and adult eye.....	28
Figure 3.1: Schematic of codon optimized TDP-43 constructs	40
Figure 3.2: Misexpression of codon optimized TDP-43 using GMR-GAL4 driver induces robust phenotype in the external eye	41
Figure 3.3: Misexpression of codon optimized TDP-43 induces depigmentation and irregularities in bristles as compared to existing human wild-type TDP-43 lines.....	43
Figure 3.4: Misexpression of codon optimized TDP-43 leads to wing expansion defects and swelling, as well as singed and loss of bristles in the <i>Drosophila notum</i>	45
Figure 3.5: Codon-optimized TDP-43 transgenic fly expresses higher levels of protein.....	47
Figure 3.6: Codon-optimized TDP-43 transgenic flies show robust mislocalization of TDP-43 to the cytoplasm and form aggregates in larval eye discs	49

Figure 4.1: TDP-43 misexpression causes altered morphology of the photoreceptor neurons in adult retina	63
Figure 4.2: TDP-43 misexpression causes degeneration and functional disruption of the photoreceptor neurons in the adult retina.....	65
Figure 4.3: TDP-43 misexpression leads to an increase in lysosomal vacuoles	67
Figure 4.4: TDP-43 misexpression induced vacuoles are positive for autophagy markers	68
Figure 4.5: TDP-43 misexpression causes changes in the levels of proteins involved in the mTOR signaling pathway	70

CHAPTER I: TDP-43 MEDIATED NEURODEGENERATION

1.1 TDP-43 Proteinopathies

Amyotrophic lateral sclerosis

Amyotrophic lateral sclerosis (ALS) is more commonly known as Lou Gehrig's disease in the United States, named after the famous baseball player who was diagnosed with the disease in the late 1930s. According to National Institute of Health studies, each year approximately 5000 people are diagnosed with this disease. It is a progressive motor neuron disease that specifically affects motor neurons involved in the control of voluntary movements. Particularly, the disease affects the upper motor neurons in the cerebral cortex and lower motor neurons in the medulla and the anterior horn of the spinal cord (Sabatelli et al., 2013). Clinical symptoms of this disease start with muscle weakness in the limbs and progress to the respiratory system. The leading cause of death in these patients is respiratory failure (Gordon, 2013). Once patients are diagnosed, they can survive somewhere between 2 to 5 years based on disease progression (Gordon, 2013). ALS can be inherited, as there are many familial cases of ALS. However, it is not just a familial disease; there are many cases of sporadic ALS. The familial ALS only accounts for a subset of these cases, while a majority of the cases of ALS are sporadic. Many of these familial cases have led researchers to identify specific genes that are involved in this disease. Among these genes, mutations in superoxide dismutase 1 gene (*SOD1*), TDP-43 gene (*TARDBP*), fused in sarcoma gene (*FUS*) and *C9ORF72* genes account for the

majority of familial cases (Gordon, 2013; Sabatelli et al., 2013). In addition, mutations in Vesicle-associated membrane protein-associated protein B/C gene (*VAPB*), charged multivesicular body protein 2B gene (*CHMP2B*), valosin-containing protein gene (*VCP*), ubiquilin-2 gene (*UBQLN2*), and p62/sequestosome 1 gene (*SQSTM1*) have also been linked to familial ALS (Sabatelli et al., 2013).

Frontotemporal lobar degeneration

Frontotemporal lobar degeneration (FTLD) is another progressive and degenerative disease that effects the frontal and temporal lobes (Riedl et al., 2014). Unlike ALS, FTLD is known to cause dementia and was previously called frontotemporal dementia. It is one of the most common types of dementia other than Alzheimer's disease. Due to the large variations in the subtypes of FTLD, the nomenclature was changed to include all of them under the same umbrella of FTLD. The different subtypes of FTLD are based on their symptoms and the component and pathology of the inclusion bodies. These subtypes include the behavioral variant FTLD, semantic dementia, progressive non-fluent aphasia, and FTLD with motor neuron disease (FTLD-MND), which is similar to ALS (Pan and Chen, 2013). These are considered to be on a spectrum of disorders due to considerable overlap among these subtypes. Based on the type of neuropathological proteins that are present in the inclusion bodies, FTLD-MND can be further subtyped into FTLD-Tau, FTLD-TDP or FTLD-FUS. Despite having these proteins in the inclusion bodies, no disease mutations have been

linked to either TDP-43 or FUS (Pressman and Miller, 2013). The most predominant among these is FTLTDP, which is induced by wild type TDP-43 in sporadic cases. To date, the only genetic mutations that have been associated with FTLTDP are microtubule associated protein tau gene (*MAPT*), valosin-containing protein gene (*VCP*), and charged multivesicular body protein 2B gene (*CHMP2B*) (Pan and Chen, 2013).

Diagnosis and current treatments

Currently, the diagnosis of ALS is limited to very few biomarkers that indicate neuronal loss and neuroinflammation in cerebral spinal fluid (CSF). In CSF from ALS patients, TDP-43 protein appears in a lower concentration compared to normal patient samples (Turner et al., 2013). Certain cytokines, including interleukins 2, 6, 10 and 15, which are involved in neuroinflammatory pathways, appear at a higher concentration in ALS patients (Turner et al., 2013). In addition to CSF biomarkers, muscle biomarker Nogo-A is strongly expressed in ALS patients (Turner et al., 2013). Neurophysiological testing using electromyography (EMG) that assesses nerve conduction can also help diagnose ALS (Turner et al., 2013). However, EMG is not a very effective way to monitor disease progression. Magnetic resonance imaging (MRI), used for structural imaging of the brain, has been widely used to diagnose ALS despite its limitations. ALS and FTLTDP patient brains show atrophy in the motor cortex in MRI scan (Pan and Chen, 2013; Turner et al., 2013). Recently, functional MRI (fMRI) studies, in addition to structural MRI scans, have helped demonstrate structural

and functional connectivity in ALS and FTLN brains and are a promising new method to diagnose these diseases (Turner et al., 2013). Moreover, similar to other neurodegenerative diseases like Alzheimer's and Parkinson's disease, post mortem tissues showing ALS pathology remain a concrete way to diagnose ALS. Similar to diagnostic biomarkers, current treatments for ALS are also limited. Riluzole, an anti-glutamatergic drug that reduces excitotoxicity, is the primary drug prescribed to ALS patients (Gordon, 2013). Riluzole has been shown to slow the disease progression, but has many side effects. In addition, multidisciplinary care, nutrition and gastrostomy are all used to help relieve symptoms and treat the patients (Gordon, 2013). During later stages of the disease, most of the patients are placed on ventilatory support (Gordon, 2013). While these treatments try to address the symptoms that arise from the disease, it is not sufficient for proper treatment of the disease. Lack of therapeutic intervention is an important factor for continuation of basic research to better understand the molecular mechanism of the disease and find therapeutic targets.

TDP-43 protein at a glance

Transactive response DNA binding protein-43 (TDP-43) is encoded by *TARDBP* gene in the human genome. In recent years, TDP-43 has been identified as one of the major components of the inclusion bodies in the brain of patients with FTLN associated with tau-negative and ubiquitin-positive inclusions and ALS (Lee et al., 2011; Mackenzie and Rademakers, 2008;

Neumann et al., 2006), among other neurodegenerative diseases (Arai et al., 2009; Hasegawa et al., 2007; Higashi et al., 2007). TDP-43 was first identified in HIV-1 virus as a transcriptional repressor (Ou et al., 1995). TDP-43 is a highly conserved, ubiquitously expressed protein that contains two RNA recognition motifs, RRM1 and RRM2, a glycine-rich region, a nuclear localization signal and a nuclear export signal; illustrated in **Figure 1.1** (Ayala et al., 2005; Buratti et al., 2005; Chen-Plotkin et al., 2010; Gendron et al., 2010). Since its discovery, many researchers have studied the protein to identify its function. The exact function of TDP-43 is still unknown, however it is known to be involved in DNA/RNA binding, RNA metabolism, particularly in the regulation of RNA levels, RNA trafficking and splicing activity. It has recently been identified that TDP-43 preferentially binds to introns, 3' untranslated regions and non-coding RNAs in the transcriptome, as well as a UG repeat motif in single-stranded RNA (Ayala et al., 2005). The glycine-rich region is involved in alternative RNA splicing and associate with the heterogeneous nuclear ribonucleoprotein (hnRNP) family of proteins (Buratti et al., 2005).

TDP-43 in neurodegeneration

Both familial and sporadic cases of these diseases have been associated with mutations in the TDP-43 gene. Most of the dominant missense mutations are present in the glycine-rich domain of TDP-43 (Lee et al., 2011; Nonaka et al., 2009). However, most of the sporadic cases of ALS and FTLN involve non-mutant, wild type TDP-43 mediated neurodegeneration. The predominance of

sporadic cases in these diseases, therefore, makes it an important task to better understand the mechanism of TDP-43 related pathogenesis that is independent of any dominant mutations. In the diseased state, TDP-43 is found to be ubiquitinated and phosphorylated, along with the presence of truncated C-terminal fragments and insoluble inclusions (Bugiani, 2007; Chen-Plotkin et al., 2010; Cohen et al., 2011; Gendron et al., 2010). Most importantly, the distinctive pathology of TDP-43 mediated neurodegeneration involves its mislocalization to the cytoplasm and the loss of normal nuclear expression (Lee et al., 2011; Neumann et al., 2006).

The mechanism by which TDP-43 triggers neurodegeneration is still unknown. Many of these disease specific mutations have been linked to formation of toxic TDP-43 aggregates that mediate neurodegeneration. To date, TDP-43 mediated toxicity and disease pathology have been implicated to occur via its susceptibility to form these toxic protein aggregates via protein-protein interaction, hyperphosphorylation, ubiquitination, and cleavage of the prion-like c-terminal fragments (Johnson et al., 2009). In addition, the increased load of toxic protein aggregates have been suggested to cause a defective protein degradation system, including autophagy and the ubiquitin proteasome system (Gendron and Petrucelli, 2011; Rubinsztein, 2006). Despite all the recent studies, the current knowledge regarding the exact mechanism of action of TDP-43 mediated neurodegeneration remains unclear.

1.2 Animal Models for TDP-43 Proteinopathies

In order to better understand and study TDP-43 proteinopathies, many animal models have been generated using both vertebrate and invertebrate organisms. To study TDP-43 in mammalian systems, many transgenic animal models have been generated in mice and rats (Gendron and Petrucelli, 2011). The majority of these models report increased ubiquitin staining or inclusions that are a major hallmark of TDP-43 mediated pathology. Many of these also report loss of nuclear TDP-43 functions or the presence of cytoplasmic TDP-43 (Igaz et al., 2011; Stallings et al., 2010; Tsai et al., 2010; Wegorzewska et al., 2009; Xu et al., 2010). Additionally, toxic TDP-43 cleavage products are present in a few of these models (Stallings et al., 2010; Tsai et al., 2010; Wegorzewska et al., 2009). Almost all of the reported animal models show some kind of neurodegenerative phenotype in cortical and motor neurons (Wegorzewska et al., 2009), in axons and neurons of the spinal cord (Xu et al., 2010), in Purkinje cell along with loss of CA3 hippocampal neurons (Wils et al., 2010), loss of neurons in hippocampal dentate gyrus and neocortex (Igaz et al., 2011) and decreased hippocampal volume (Tsai et al., 2010) among many others. The animal models of TDP-43 that are currently available vary in which promoter is utilized to drive the expression of the transgene. Some of these models use PrP promoter to drive wild type and mutant TDP-43 constitutively, while others use CaMKII and TRE (CaMKII-tTA) drivers to express wild type, mutant and partially deleted constructs of TDP-43 both constitutively and conditionally (Igaz et al., 2011; Stallings et al., 2010; Tsai et al., 2010; Wegorzewska et al., 2009). In

addition to these mammalian models, there are also many invertebrate models of TDP-43 available. *Caenorhabditis elegans* models that overexpress human TDP-43, as well as nematode ortholog TDP-1, are used to study TDP-43 mediated mechanism for neurodegeneration. These *C. elegans* models show neuronal toxicity, motor defects and TDP-43 phosphorylation mediated toxicity of wild type and mutant TDP-43 in the motor neurons (Ash et al., 2010; Liachko et al., 2010; Vaccaro et al., 2012; Zhang et al., 2012). A loss of function model for zebrafish ortholog of *TARDBP* shows locomotion defects with shorter motor axons. Along with *C. elegans* and zebrafish (Schmid et al., 2013), *Drosophila melanogaster* models are also used to study the molecular mechanism of TDP-43 in neurodegeneration and are discussed in more detail in chapter III.

1.3 *Drosophila* Models for Neurodegeneration

Drosophila melanogaster, commonly known as the fruit fly, has a very short life cycle. Under laboratory conditions, flies can live up to 30-40 days on average. Adult females lay embryos that undergo larval and pupal stages and develop into adult flies in approximately 9-10 days at room temperature. *Drosophila* is fairly inexpensive and easy to maintain in the laboratory. There are many advantages in using a *Drosophila* model to study neurodegeneration. Despite having a much smaller genome size compared to humans, many of the human genes have fly homologs, as they are evolutionarily conserved (Bellen et al., 2004). In addition, many of the important signaling pathways are also conserved between fly and human, such as the Notch pathway, the wingless/Wnt

pathway and the transforming growth factor- β (TGF- β)/decapentaplegic pathway (Adams et al., 2000). *Drosophila* has been studied in many fields of biological sciences for many years and as a result there are various tools that are widely available (Bier, 2005). Many of these tools allow for genetic manipulation that can help us study the molecular functions of genes in an *in vivo* system. There are many genetic mutants and genetic knockdown using RNAi allows for loss of function studies. On the other hand, many tools allow overexpression of certain genes for gain of function studies (Bilen and Bonini, 2005; Muqit and Feany, 2002; Sang and Jackson, 2005). One such tool is the GAL4/upstream activation sequence (UAS) binary system (Brand and Perrimon, 1993). The yeast transcription activator protein GAL4 can bind to the UAS and allow the transcription of the gene attached to the UAS in a tissue specific manner (**Figure 1.2**). The direct promoter fusion construct is another way to overexpress a certain gene. The selected gene can be directly subcloned into a vector containing the tissue specific promoter and drive its expression. Many of these vectors are easily available through the *Drosophila* genomic resource center (DGRC). All of these reasons contribute significantly to the generation of many fly models to study neurodegeneration.

***Drosophila* eye as a model**

Many neurodegenerative disease models utilized the *Drosophila* eye as a tissue of choice for the study of gene expression. The fly eye development occurs in multiple stages that are highly regulated by important signaling

pathways and are well characterized. The *Drosophila* compound eye is a highly specialized structure that is composed of ~750-800 ommatidia. Each ommatidium consists of 8 photoreceptor neurons that are similar to mammalian photoreceptor neurons. In addition there are different types of supporting cells that include 4 cone cells, primary, secondary and tertiary pigment cells and interommatidial bristle cells (Carthew, 2007; Kumar, 2001, 2011; Tsachaki and Sprecher, 2012). The differentiation of these different types of cells from epithelial precursor cells occurs in a spatial and temporal manner throughout eye development. The specification of the compound eye requires seven nuclear factors or eye specific genes that are evolutionarily conserved between fly and human. These factors form a complicated regulatory network that determines the fate of the precursor cells (Carthew, 2007; Kumar, 2011). The initial phase of eye development occurs early in the larval stage. In the eye imaginal disc, the transition from proliferation state to differentiation state occurs at a dorsoventral groove, called the morphogenetic furrow. During the pupal stage, cone cells recruit primary pigment cells. After differentiation, the cone cells and the primary pigment cells expand further while constraining the interommatidial precursor cells (IPCs). The IPCs further differentiate into the secondary and tertiary pigment cells, as well as interommatidial bristle cells (Carthew, 2007; Kumar, 2001; Tsachaki and Sprecher, 2012). A large portion of *Drosophila* genes are involved in this intricate process of development.

A gene that is expressed in the eye can interact with the specific pathways involved in the developmental process. Such interactions can show a phenotype in either the external or internal structures of the adult retina. The fly eye is dispensable and not required for its survival under laboratory conditions. This has a huge advantage when modeling neurodegeneration in the eye, as many of these toxic proteins induce severe degenerative phenotypes (Muqit and Feany, 2002; Sang and Jackson, 2005). Despite causing toxicity, these flies are able to survive into adulthood and can be used to create stable lines expressing a desired gene. In addition, the architecture of the external fly eye is easily visible under light microscopes, allowing convenient detection of any phenotype that might arise from expressing or knocking down a certain gene. These phenotypes are often easily scored under light microscopes and allow for detection of any chemical or genetic modifiers of a gene expressed in the retina.

Neurodegeneration in flies

One of the earliest models of neurodegeneration in *Drosophila* studied expanded polyglutamine proteins. Bonini and colleagues reported glutamine-repeat expansion in a Spinocerebellar ataxia type 3 (SCA3) model that showed degenerative phenotypes along with nuclear inclusions in the fly retina (Warrick et al., 1998). Separately, Jackson and colleagues reported that a novel *Drosophila* model of polyglutamine –expanded human Huntington protein, known to cause Huntington's disease, showed degenerative phenotypes in the photoreceptor neurons of the retina (Jackson et al., 1998). They also showed

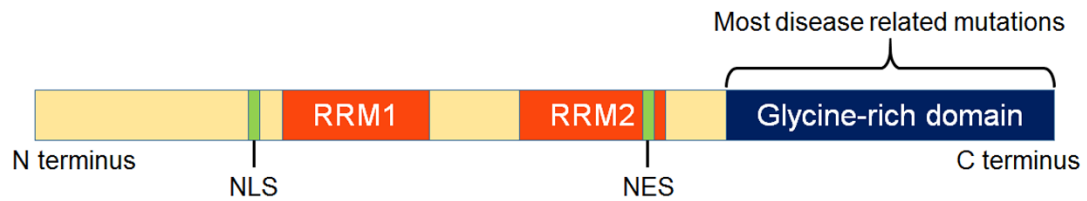
that *Drosophila* Apaf-1 can block polyglutamine aggregation and pathology, while Bonini and colleagues showed that neurodegeneration mediated by polyglutamine can be suppressed by the hsp70, a known molecular chaperone (Sang et al., 2005; Warrick et al., 1999). Alzheimer's disease models with human tau were also reported to induce degenerative phenotypes in flies. Jackson and colleagues reported that human wild type tau interacted with wingless signaling pathway to induce neurofibrillary tangles (Jackson et al., 2002). Since then, many new *Drosophila* models for Alzheimer's disease related neurodegeneration have been generated that include tau, amyloid-beta and gamma-secretase models (Finelli et al., 2004; Fulga et al., 2007; Guo et al., 2003; Iijima et al., 2004; Jackson et al., 2002; Kosmidis et al., 2010). Tauopathies have been extensively studied in *Drosophila*. There are many studies that look at genomic screens in a tauopathy model to identify genetic modifiers of tau (Ambegaokar and Jackson, 2011; Karsten et al., 2006; Shulman and Feany, 2003). In addition, tau hyperphosphorylation has also been implicated to cause neurotoxicity (Chatterjee et al., 2009; Steinhilb et al., 2007a; Steinhilb et al., 2007b). The role of TOR mediated cell-cycle activation and autophagy has also been studied in tauopathy models of neurodegeneration (Khurana et al., 2006).

The first *Drosophila* model of Parkinson's disease was reported by Feany and colleagues, showing wild type and mutant α -synuclein mediated intraneuronal inclusions and neurodegeneration in flies (Feany and Bender, 2000). There are also models of mutant human Parkin that causes toxicity

through selective loss of dopaminergic neurons in flies (Sang et al., 2007). Parkin mutants have been found to be responsible for mitochondrial pathology and muscle degeneration in flies (Greene et al., 2003). Moreover, Pink-1, also involved in Parkinson's disease, has been shown to interact with Parkin and is required for mitochondrial function (Clark et al., 2006). Over the last decade, many other neurodegenerative disease models in *Drosophila* have been reported. Some of these models of neurodegenerative proteins, which include ataxin-3, a protein involved in spinocerebellar ataxia (Bilen and Bonini, 2007), VAP33 (Ratnaparkhi et al., 2008) and SOD1 (Watson et al., 2008), are involved in ALS. There have been many reports of TDP-43 proteinopathy models in *Drosophila* that study both the fly homologue and the human TDP-43 protein. Chapter III contains a more detailed overview of these *Drosophila* models of TDP-43 proteinopathies. The genetic tools of *Drosophila* have allowed for extensive studies on neurodegenerative diseases. Many of these have tried to understand the molecular mechanism and performed genetic screens to help us identify the role these toxic proteins play in neurodegeneration.

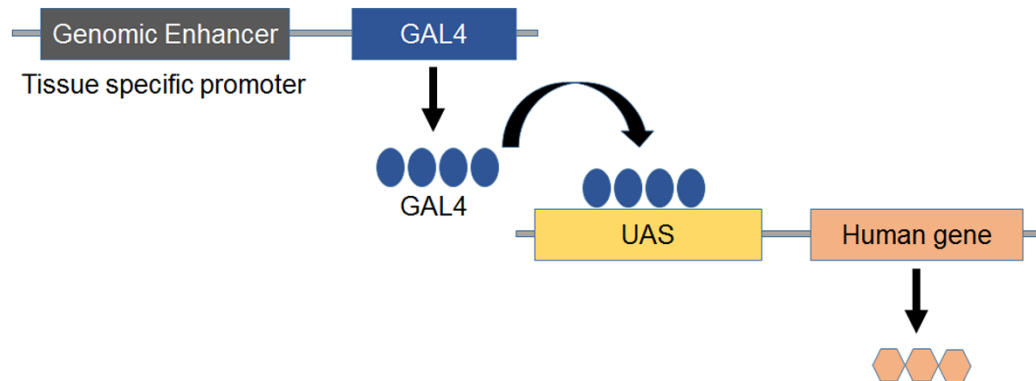
FIGURES

Figure 1.1. Schematic of the TDP-43 protein



The ubiquitously expressed TDP-43 protein contains two RNA recognition motifs (RRM), a glycine-rich region, a nuclear localization signal (NLS), and a nuclear export signal (NES). The majority of the disease related mutations are found in the glycine-rich region near the c-terminus.

Figure 1.2. The GAL4-UAS binary system



The GAL4-UAS binary system allows transcription and expression of a gene of interest in the desired tissue or region in spatio-temporal manner. In flies expressing the GAL4 driver and the UAS sequence, the tissue specific promoter will drive the expression of the GAL4 protein. The GAL4 protein then binds to the UAS sequence and activates the expression of the desired gene downstream of the UAS sequence.

CHAPTER II: MATERIALS AND METHODS

2.1 Fly Stocks and Genetics

Drosophila is easily maintained under laboratory conditions in bottles and vials containing fly food media. The flies were given the standard *Drosophila* Jazzmix medium (Applied Scientific, Fisher Scientific, Pittsburgh, PA, USA) that contains cornmeal, yeast and sugar. For long term storage, the food was kept in 4°C temperature. All flies were maintained and most crosses were set at room temperature (22°C) unless otherwise specified.

Codon optimized TDP-43 flies

The codon optimized TDP-43 gene was synthesized from DNA2.0. *Drosophila* kozak sequence was added upstream of the start codon for the TDP-43 gene. These constructs were subcloned into the modified *Drosophila* pExpress upstream activation sequence (UAS) expression vector (pEx-UAS) and *glass* (pEx-*gl*) expression vectors (Exelixis, San Francisco, CA, USA). These vectors contain an Ampicillin resistance sequence, origin of replication, inverted repeat sequence and a mini w⁺ background, all upstream of the Hsp70 TATA box promoter. Downstream of the UAS or *glass* sequence, the multi-cloning site is present and the codon optimized TDP-43 constructs were subcloned into that region using the restriction endonucleases Not1 and Xba1 sites (**Figure 2.1**). The expression vectors containing the codon optimized TDP-43 were then microinjected into the flies to obtain transgenic flies (BestGene, Chino Hills, CA,

USA). We obtained multiple lines of the codon optimized flies. However, upon initial observations, only a subset of those were used in most of the experiments.

We have made a stable line expressing the TDP-43 gene under the SevEP-GAL4 driver (expressed in R7 and R8 photoreceptor neurons) (Therrien et al., 1999). The SevEP-GAL4 driver was recombined with UAS TDP-43^{CO} to obtain stable transgenic flies expressing w¹¹¹⁸;SevEP-GAL4,UAS-TDP-43^{CO}/CyO;+. In addition, we used the GMR-GAL4 (eye specific) driver on the X-chromosome to express a UAS containing gene in addition to codon optimized TDP-43 in the retina. GMR-GAL4 driver was placed in trans to the *g^l*-TDP-43^{CO} expressed on the second chromosome to generate GMR-GAL4;*g^l*-TDP-43^{CO}/CyO transgenic flies.

Genotypes

Flies expressing human wild type TDP-43 using the UAS promoter (Lu et al., 2009) were obtained from Dr. Fen-Biao Gao (University of Massachusetts, Worcester, MA, USA). E_q-GAL4 (bristle driver) (Tang and Sun, 2002) was obtained from Hugo J. Bellen (Baylor College of Medicine, Houston, TX). The following stocks were obtained from Bloomington Stock Center (Bloomington, Indiana University, IN, USA): w¹¹¹⁸;UAS-LacZ, w¹¹¹⁸,GMR-myr-mRFP, y¹,w¹¹¹⁸;Sp/CyO;eGFP-ATG5, y¹,w¹¹¹⁸;UASp-GFP-mCherry-ATG8,GMR-GAL4(X) (eye specific), w¹¹¹⁸;SevEP-GAL4 (R7 and R8 in photoreceptor cells), y¹,w¹¹¹⁸;Rh1-GAL4/CyO (expressed in R1-R6 photoreceptor cells),

w¹¹¹⁸,beadex^{MS1096}-GAL4 (wing driver), w¹¹¹⁸;Scabrous-GAL4 (sensory organ precursor and wing discs driver), y¹,w^{*}; CCAP-GAL4 (driver expressed in CCAP/bursicon neurons in ventral nerve cord and subesophageal ganglion in adult brain).

2.2 Immunohistochemistry

The immunohistochemistry experiments were performed in the adult retina and imaginal eye discs from third instar larvae. The dissections were done under a light microscope (Leica Microsystems, Buffalo Grove, IL, USA). Using fine forceps and tungsten needles (Fine Science Tools, Foster City, CA, USA), the third instar larval eye discs were dissected in 1X PBS solution. Following dissections, the imaginal eye discs were immediately transferred and fixed in 4% paraformaldehyde for 1 hour on ice. The tissue was blocked in 0.8% PBS+Triton-X+BSA for 2 hours at room temperature (22°C). Immediately after blocking, the tissue was incubated with primary antibody overnight at 4°C. The next day, the tissue was washed in 0.1% PBS+Triton-X 5 times in 10 minutes intervals. Next, the tissue was incubated in secondary antibody for 2 hours at room temperature (22°C). The tissue was washed again in 0.1% PBS+Triton-X 5 times in 10 minutes intervals. Finally, the tissue was mounted on glass slides with Vectashield (Vector Laboratories, Burlingame, CA, USA), covered with a coverslip and sealed with nail polish.

The adult eye was stained in a similar protocol with some modifications. The fly heads were decapitated and a cut was made along the edges of the adult retina with a blade. The retina was immediately transferred to 4% PFA on ice and kept for 1 hour. After approximately 45 minutes of incubation, the remnants of the medulla, the lamina, excess tissue surrounding the cornea were removed. Following incubation in fixative, in an additional step, the adult retina was washed in 0.5% PTX for 3 hours to reduce autofluorescence. The washes following antibody incubation were done in 0.5% PBS+Triton-X. To prevent damages to the tissue, the adult eye was mounted in a well created by two coverslips on the glass slide, covered with an additional coverslip and sealed with nail polish. The tissues were imaged the next day using a confocal microscope. The z-stack images were obtained at 0.5 μ M difference and analyzed using LSM Image Browser and ImageJ software from NIH. **Figure 2.2** illustrates the specific area of the tissue that was imaged.

Tissues were stained with following antibodies: mouse monoclonal anti-TDP-43 antibody (1:500, Abcam, Cambridge, MA, USA), rabbit polyclonal anti-TDP-43 antibody (1:500, Proteintech, Chicago, IL, USA), rat monoclonal anti-Elav (1:20, DSHB, University of Iowa, Iowa City, IA, USA), mouse monoclonal anti-GFP (1:400, Millipore, Billerica, MA, USA), Alexa Fluor 633-conjugated Phalloidin (1:30, Invitrogen, Grand Island, NY, USA), Alexa Fluor 488 conjugated chicken anti-rat (1:400, Invitrogen, Grand Island, NY, USA) Alexa Fluor 568 conjugated

goat anti-rabbit (1:400, Invitrogen, Grand Island, NY, USA) and Alexa Fluor 568 conjugated goat anti-mouse (1:400, Invitrogen, Grand Island, NY, USA).

2.3 Immunoblotting

The protein samples were collected from fly eye expressing the human TDP-43 protein. Approximately 50 fly heads were harvested and homogenized on ice for 1 min in homogenization buffer (10mM Tris-HCl, 0.8 M NaCl, 1 mM EGTA, pH 8.0 and 10% sucrose) along with 1X PhosSTOP phosphatase and 1X cOmplete protease buffer (Roche Applied Science, Indianapolis, IN, USA). The homogenized samples were then centrifuged at 4°C for 15 min at 18,000g. The supernatant was collected and the pellet was discarded. To prepare the sample, equal parts of the supernatant and Laemmle sample loading buffer including β -mercaptoethanol (Bio-Rad, Hercules, CA, USA) was added for each sample. For higher molecular weight species detection, the fly head were homogenized in 1X PBS along with the same protease and phosphatase inhibitors. Also, non-reducing sample loading buffer (Nupage sample buffer, Life Sciences, Grand Island, NY, USA) was added to the supernatant without β -mercaptoethanol.

Following a brief pulse centrifugation, samples were loaded on 4-20% SDS-PAGE gels (Bio-Rad, Hercules, CA, USA) for electrophoresis in 1X Tris-Glycine+SDS buffer. To determine the molecular weights, the Precision Plus Protein Dual Color Standards (Bio-Rad, Hercules, CA, USA) were used. The gel electrophoresis was run at a constant 90 V for approximately one and half hours.

Immediately after the gel electrophoresis, the gel containing the proteins was transferred to the supported nitrocellulose membrane (Bio-Rad, Hercules, CA, USA) for 3 hours on ice. For transfer, 1X Tris-Glycine+Methanol buffer was used and it was run at a constant 200 mA. The membrane was pre-soaked in the 1X Tris-Glycine+Methanol buffer along with the filter papers for better transfer of the proteins. Following transfer, the membranes were blocked in 5% milk for 1 hour at room temperature (22°C) and incubated with primary antibodies overnight at 4°C. The next day, membranes were washed in 1X TBS+Tween 6 times in 5 minutes intervals. Immediately after, the membranes were incubated with the secondary antibody for 2 hours at room temperature (22°C). Next, the membranes were washed again in 1X TBS+Tween 6 times in 5 minutes intervals. For chemiluminescence reaction, the membranes were exposed to ECL (GE Healthcare) for 5 minutes and developed immediately after.

The following antibodies were used: mouse monoclonal anti-TDP-43 antibody (1:1000, Abcam, Cambridge, MA, USA), mouse monoclonal anti-tubulin antibody (1:1000, DSHB, University of Iowa, Iowa City, IA, USA), rabbit monoclonal phospho-4E-BP1 (Thr37/46) antibody (1:1000, Cell Signaling, Boston, MA, USA), rabbit polyclonal phospho-p70-S6K (*Dros* Thr398) antibody (1:1000, Cell Signaling, Boston, MA, USA), rabbit polyclonal phospho-AKT (*Dros* Ser505) antibody (1:1000, Cell Signaling, Boston, MA, USA), secondary anti-mouse IgG-HRP (1:2000, GE Healthcare) and secondary anti-rabbit IgG-HRP (1:2000, GE Healthcare).

2.4 LysoTracker Staining

LysoTracker staining was done using imaginal eye discs from the third instar larvae. To prepare, the LysoTracker Red DND-99 (Invitrogen) was diluted in 1X PBS solution to prepare a 100 nM solution. The larval eye discs were dissected in 1X PBS solution using a light microscope (Leica Microsystems, Buffalo Grove, IL, USA). No fixative was added to the eye discs. The tissues were stained with 100 nM LysoTracker solution for 2 minutes. This was followed by a quick 1 minute wash in 1X PBS. The tissues were mounted on a glass slide with a drop of 1X PBS solution. Vectashield was not added to the tissues. The coverslip was placed on top of it and sealed with nail polish. Only one eye disc was placed on each slide to prevent long incubation time. The tissues were visualized immediately using a confocal microscope. The z-stack images were obtained at 0.5 μ M difference and analyzed using the LSM Image Browser and ImageJ software from NIH.

2.5 Electroretinogram

ERG was recorded in external retina of 1 day old flies following previously described methods (Fabian-Fine et al., 2003; Williamson et al., 2010). Approximately 15 female flies were collected post-eclosion and the experiment was performed the next day. The flies were anesthetized in carbon dioxide and placed on their sides on a glass slide with a thin layer of Elmer's non-toxic glue. The glue helps minimize the movements of the fly. The ERG recordings were collected immediately after from the exposed right eye. Both the reference and

recording electrodes were made of glass pipettes. The electrodes were filled with 3M KCl. The slightly broken reference electrode was placed in the thorax of the fly, while the recording electrode was placed on the cornea of the eye. Using a computer controlled white light-emitting diode system (MC1500; Schott), the light stimulus was provided to the exposed retina with the electrodes. The light stimulus was provided in 1 second pulses, with a 3 second resting period in between. The data were recorded using Clampex software (version 10.1; Axon Instruments) and measured and analyzed using Clampfit software (version 10.2; Axon Instruments).

2.6 Optical Neutralization and Pseudopupil

On a glass slide, a small drop of clear nail polish was placed to mount the fly head. Female fly heads were decapitated and immediately placed on the nail polish at approximately 45° angle, so that the fly heads were at an incline with the eye pointing upwards. Once the nail polish dried, a drop of immersion oil (Cargille Labs, Cedar Grove, NJ, USA) was placed on the eye. The immersion oil allowed the eye to be optically neutralized. The glass slide was placed under a 40X oil-immersion objective. To observe the pseudopupil, light was passed from below using a condenser with a small aperture.

2.7 Microscopy

For general fly husbandry and dissection, a light microscope was used (Leica Microsystems, Buffalo Grove, IL, USA). For optical neutralization and

pseudopupil, a Nikon Eclipse 800 upright microscope (Nikon Instruments, Melville, NY, USA) was used. To obtain high resolution images of the adult eye, wing and bristle pictures, a Nikon AZ100M microscope equipped with a Nikon DS-Fi1 digital camera (Nikon Instruments, Melville, NY, USA) was used. Adult female flies were anesthetized using carbon dioxide and placed on their side on a glass slide containing clear nail polish. Only the left fly eye was imaged immediately after mounting. For the images of the bristles, the female flies were also mounted on a glass slide with clear nail polish, but on their abdomen. The left wing from adult females were cut with a fine scissor and placed on a glass slide without any adhesive. A series of high resolution images were taken as z-stacks that covered the entire depth of the tissue using the Nikon NIS-Elements AR 3.0 software. Extended depth of focus (EDF) images were obtained using the tool also called EDF that combines all the images from different z-stack planes and creates a focused image. Once the EDF images were created, a tool for volumetric visualization allowed us to obtain volumetric images that can be viewed from different angles. Images represented are visualized from the anterior end of the adult eye.

The adult flies were not prepared or dehydrated for the scanning electron microscope (SEM) images. The flies were simply anesthetized using carbon dioxide and placed on the special cylindrical mounts using clear nail polish. Similar to the colored images obtained, the flies were placed on their sides so that the left eye could be imaged. Since the flies were not prepared for long term

preservation, the eye typically collapsed within 15 minutes of mounting, losing its internal pressure and structural integrity. Therefore, only one fly was prepared at a time and imaged immediately after using the JSM-6510LV SEM (JEOL USA, Peabody, MA, USA).

For confocal images, the samples were prepared as previously described in the **2.2 Immunohistochemistry** section. The confocal images were taken with a Zeiss LSM 510 UV META laser scanning confocal microscope using 40X water and 63X oil-immersion high resolution objectives. These images were analyzed using the LSM Image Browser and NIH ImageJ software.

2.8 Quantification and Statistical Analysis

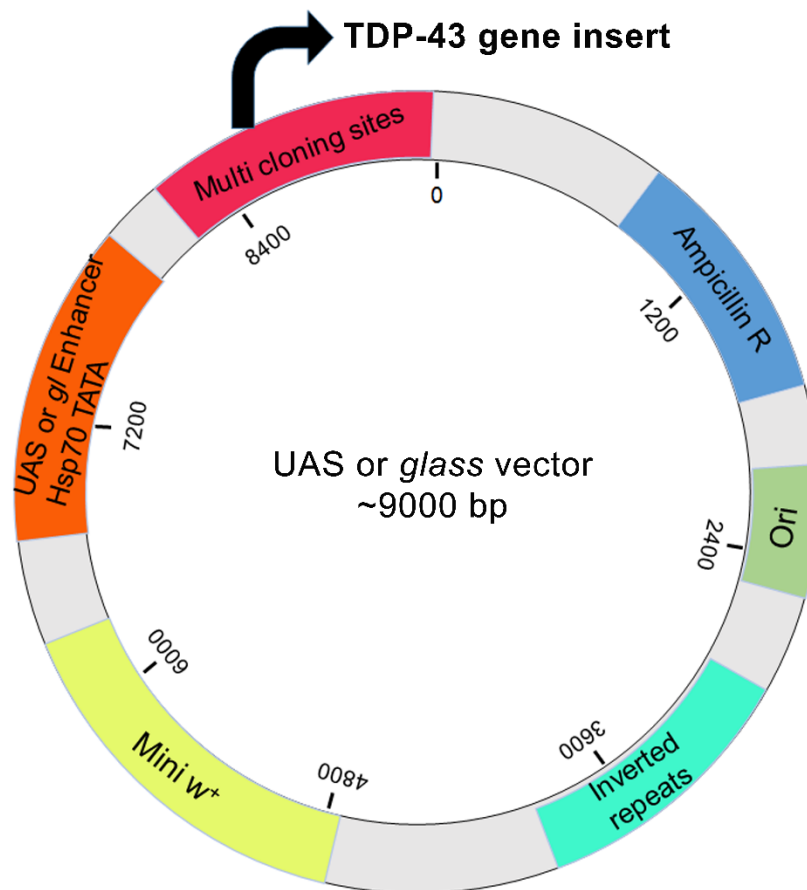
Quantification of LysoTracker staining was performed using the NIH Image J software. The z-stack projection images were corrected for background noise and converted to 8-bit images for color depth reduction. The images were then adjusted for detection threshold. Using the “analyze particles” tool for automated quantification, total number of particles were collected. The total particle count was then divided by the total area (calculated using the “measure” tool) to get the puncta count for each sample. Approximately 15 samples were used for each genotype. The histograms represent mean \pm SEM and were plotted using SigmaPlot (version 10.1) software. The statistical analysis was performed using paired Student’s t-test with two-tailed distribution of equal variance.

For the ERG quantification, the values of the on transient and depolarization were obtained using the Clampfit software. Approximately 15 female flies were used for each genotype. The calculations were made using Microsoft Excel software and the histograms represent mean \pm SEM values that were plotted using SigmaPlot (version 10.1). Using the same software, statistical analysis was performed using one-way ANOVA with Bonferroni's correction.

The quantification of immunoblots probed with different antibodies was analyzed using the ImageJ software. Using the "gels" tool under analyze, the area under the curve was measured for each individual lane. The area for each band of specific antibody was divided by the area for the corresponding band of tubulin antibody that was used as a loading control. Therefore, each antibody intensity was compared to the loading control of each individual lane. The histograms represent the mean \pm SEM for each genotype. For these data, the statistical analysis was also performed using paired Student's t-test with two-tailed distribution of equal variance.

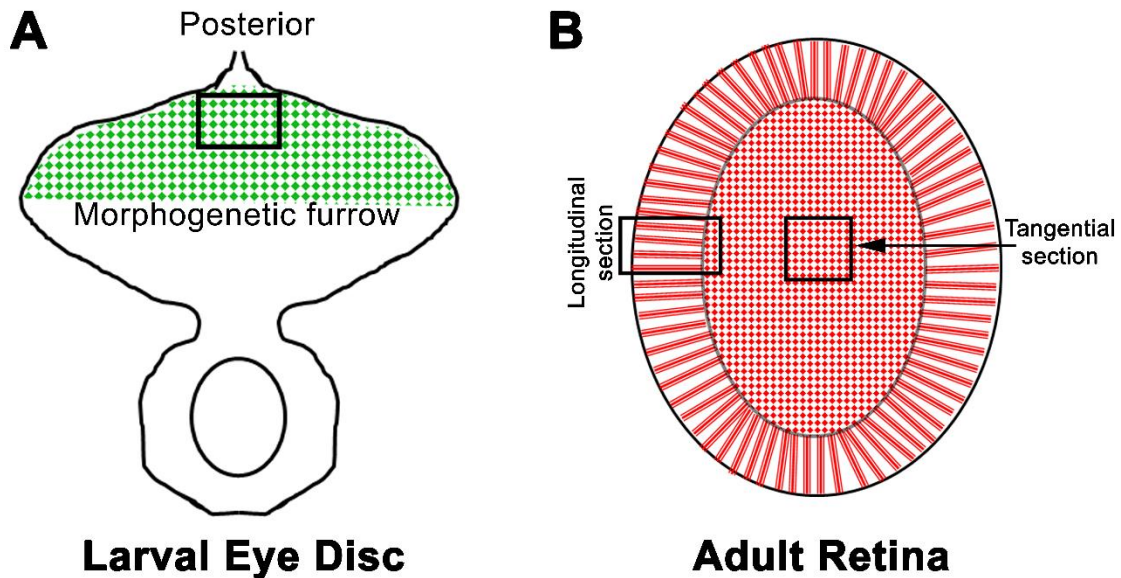
FIGURES

Figure 2.1. pExpress UAS/*glass* vector



The pExpress UAS and *glass* vectors were used to generate the codon optimized TDP-43 flies. The vectors are approximate 9000 bp in length. Along with the UAS or *glass* sequence, the vectors contain multiple regions of interest, including the ampicillin resistant sequence, origin of replication (Ori), inverted repeat sequence, mini w⁺ sequence and multi cloning sites. The TDP-43 gene was inserted into the multi cloning site using Not1 and Xba1 restriction enzymes.

Figure 2.2. Schematic of larval eye disc and adult eye



(A) The third instar larval eye disc. The morphogenetic furrow develops along the dorsal-ventral invagination. Posterior to the morphogenetic furrow, the neuronal photoreceptor cells mature and project their axons to the larval laminal plexus. The area marked by the rectangle was used to image these photoreceptor neurons. **(B)** The adult retina is a convex shaped tissue that contains the cone cells, pigment cells, interommatidial bristle cells and photoreceptor neurons that project axons to the lamina. For immunostaining, the lamina and medulla, along with the cornea, were removed. Areas marked by the rectangles were used to image the rhabdomeres/photoreceptor neurons.

CHAPTER III: ROBUST PHENOTYPES OF THE CODON OPTIMIZED TDP-43

DROSOPHILA MODEL

3.1 Introduction

Current *Drosophila* models for TDP-43 proteinopathies

There are many *Drosophila* transgenic models for TDP-43 that have been used to study the role of TDP-43 in neurodegeneration. These models include loss of function, gain of function, deletions and RNAi transgenic models. The TDP-43 ortholog of the fly is known as TBPH, which is similar to human TDP-43 in structure and function (Gendron and Petrucelli, 2011; Stallings et al., 2010; Tsai et al., 2010; Vaccaro et al., 2012; Wegorzewska et al., 2009). There are many *Drosophila* models of the fly TDP-43 as well. Among many advantages of studying transgenic fly models is tissue specific expression of the transgene. There have been many studies that looked into the mushroom bodies, motor neurons, neuromuscular junction, eye, muscle, glial and pan-neuronal expression of TDP-43 (Elden et al., 2010; Estes et al., 2011; Feiguin et al., 2009; Godena et al., 2011; Guo et al., 2011; Li et al., 2010; Lin et al., 2011; Lu et al., 2009; Miguel et al., 2011; Ritson et al., 2010). One of the earliest models to characterize TDP-43 mediated affect was studied by Gao and colleagues that reported that TDP-43 was essential to maintain the structural integrity of dendrites and a loss of function mechanism compromised the diseased neurons (Lu et al., 2009). Similarly, Baralle and colleagues also reported the loss of function mechanism for fly homologue of TDP-43 induced deficiency in locomotion and anatomical

defects of the neuromuscular junctions (Feiguin et al., 2009). To identify possible disease mechanism, loss of the normal function of TDP-43 has also been linked to a downregulation of histone deacetylase-6 (HDAC6), which is known to regulate chromatin structure, bind to ubiquitinated proteins and is required for the formation of stress granules (Fiesel et al., 2010). Wu and colleagues studied an overexpression model for human TDP-43 and found that increased expression of TDP-43 is neurotoxic and led to aberrant regulation of TDP-43 (Li et al., 2010).

It has recently been shown that TDP-43 interacts with many different RNAs using CLIP-sequence methods. Some *Drosophila* models of TDP-43 have shown specific proteins that interact with TDP-43 and contribute to disease related mechanism. Gitler and colleagues showed that TDP-43 interacts with ataxin 2, a protein known to cause spinocerebellar ataxia type 2, and proposed a possible disease mechanism (Elden et al., 2010). Another TDP-43 interacting protein, ubiquilin 1, has been shown to increase the severity of TDP-43 mediated toxicity in a cell-autonomous mechanism (Hanson et al., 2010). Disease specific mutant TDP-43 has been shown to interact with valosin-containing protein (VCP), a ubiquitin segregase protein involved in neurodegeneration, and mediate a gain of function mechanism for toxicity (Ritson et al., 2010). Mutant *Drosophila* TDP-43 has also been reported to regulate the expression of micro RNAs, specifically miR-9a, which proposes a novel role of TDP-43 in neuronal specification (Li et al., 2013). In the *Drosophila* neuromuscular junction, Feiguin and colleagues have shown that mutant TDP-43 interacts with Futsch/MAP1B RNA to regulate

its level and cause synaptic defects (Godena et al., 2011). In addition to these potential interactions, Panday and colleagues have shown TDP-43 to possibly interact with FUS/TLS, a protein also linked to ALS (Lanson et al., 2011). Separately, McCabe and colleagues reported that FUS and TDP-43 function together *in vivo* and the combined molecular pathways involving these proteins might be disrupted in ALS (Wang et al., 2011).

Phosphorylation of TDP-43 has also been studied in *Drosophila* models of TDP-43 proteinopathies. Tu and colleagues have suggested that hyperphosphorylation serves as a defense mechanism against TDP-43 aggregation (Li et al., 2011). However, Jackson and colleagues have shown that disease specific mutant TDP-43 gets phosphorylated by casein kinase I ϵ , CKI, which leads to increased oligomerization and toxicity *in vivo* (Choksi et al., 2014). Moreover, Perez and colleagues, identified CKI inhibitors to be a potential therapeutic drug (Salado et al., 2014).

***Drosophila* model with codon optimized TDP-43**

We have generated multiple codon optimized human wild-type TDP-43 transgenic flies to investigate TDP-43 mediated neurodegeneration. Typically, for protein translation, there is at least one codon (3-base pair sequence) that codes for a specific amino acid in a polypeptide chain generated from an mRNA transcript. For some amino acids, there are more than one codon that can code for that specific amino acid. Previously, it has been shown that efficiency of

mRNA transcription or translation depends on the cellular environment and altering the codon used to code for a particular amino acid can also affect the protein translational efficiency. In *Drosophila*, codon bias, where certain codons are “preferred” over others, can lead to an optimized expression of protein. To generate these codon optimized flies, certain coding regions have been altered in the human *TARDBP* gene for optimal *Drosophila* cellular environment. These codon optimized transgenic lines express TDP-43 protein that is identical in amino acid sequence to human TDP-43 protein, only the codons in the DNA/RNA are altered for optimization of the *Drosophila* transcriptional and translational machinery.

The codon optimized transgenic lines utilize the yeast GAL4/UAS binary system, as well as *glass* promoter direct fusion construct specifically to study TDP-43 mediated effects in *Drosophila* retina (**Figure 3.1 A-B**). The human TDP-43 gene is inserted in either the second or third chromosome of the fly. TDP-43 is expressed in a mini *w⁺* background and can easily be maintained using genetic balancers for second and third chromosomes. We have generated multiple versions of both the *glass* direct fusion construct and the GAL4 driven UAS constructs. The codon optimization allows for a better expression of human TDP-43 gene in a fly model. While all the currently available models allow TDP-43 to be studied in an in vivo system, many of these do not show robust phenotypes for wild type TDP-43. Currently, most proteins are known to interact with mutant

forms of TDP-43, limiting the understanding of TDP-43 pathology mediated by wild type TDP-43 in sporadic cases of ALS and FTLD.

3.2 Results

Codon optimized TDP-43 misexpression in the *Drosophila* eye causes robust phenotypes

In order to study the effects of TDP-43 misexpression, initially we expressed TDP-43 in the *Drosophila* eye using 2 different eye-specific *glass* multimer reporter (GMR)-GAL4 drivers: GMR-GAL4 on the X-chromosome (Freeman, 1996) and GMR-GAL4 on the second chromosome (summarized in **Table 3.1**). The TDP-43 misexpression using the eye specific promoter utilizes only one copy of the TDP-43 gene. All 8 different lines generated with the UAS vector were tested at two different temperatures. We found that when using both of the drivers at lower temperature (18°C), some lines show lethality. However, some of the lines have some progeny that escape and they show a robust eye phenotype that consists of depigmentation, irregularities in interommatidial bristles, loss of volume leading to flattened surface and necrotic patches or hypermelanization that worsens with age (**Figure 3.2**). At a higher temperature (25°C), most of the lines show lethality upon TDP-43 misexpression (**Table 3.1**). Despite only having one copy of the gene expressed, the expression of the TDP-43 protein leads to lethality in flies. To bypass such strong expression of the protein, we generated direct fusion constructs (with eye-specific *glass* promoter) that bypass the GAL4-UAS system, as well as used milder GAL4 drivers to

induce lesser expression of TDP-43. All of these lines utilize only one copy of TDP-43 gene to drive the expression and are viable.

Unlike the previously characterized human wild-type transgenic flies that we and others have studied, these misexpressed codon optimized TDP-43 transgenic flies show a robust eye phenotype. At 10 days post-eclosion, TDP-43 expressed using the *glass* direct promoter fusion constructs causes depigmentation, mild roughness, disruption of polarity and loss of interommatidial bristles (**Figure 3.3 D and H**). The codon optimized TDP-43 misexpressed using a different eye promoter that is milder and only expresses in a subset of photoreceptor neurons (R3, R4 and R7) and in cone cells, *Sevenless* EP-GAL4 (SevEP-GAL4), shows a similar, but milder phenotype of the eye (**Figure 3.3 C and G**). The previously reported human TDP-43 transgenic flies, expressed in the fly eye using the GMR-GAL4 driver (**Figure 3.3 B and F**) did not show a robust eye phenotype and appear to be similar to the wild-type Canton S flies (**Figure 3.3 A and E**). As mentioned before, the codon optimized TDP-43 expressed with GMR-GAL4 driver shows lethality (**Figure 3.2**).

The phenotype observed with heterozygous *g/-*TDP-43 codon optimized flies is age dependent. At 1 day post-eclosion, the phenotype seems milder (**Figure 3.3 J**), but it worsens by day 10 (**Figure 3.3 D and H**). Unlike the heterozygous expression of TDP-43, the homozygous codon optimized *g/-*TDP-43 flies are lethal with few escapers that die within 3 to 4 days post-eclosion. At 1

day post-eclosion, the homozygous flies show a very strong phenotype with apparent necrotic patches or hypermelanization that worsen with age (**Figure 3.3 K**). Both hetero- and homozygous codon optimized TDP-43 flies appear to have lesser eye volume than wild-type Canton S flies (**Figure 3.3 L-N**). These observed phenotypes indicate that codon optimized wild-type TDP-43 transgenic flies have a more robust phenotype when expressed in the eye compared to human wild-type TDP-43 transgenic flies.

Codon optimized TDP-43 misexpression in wings causes inflation defects and loss of bristles in *Drosophila notum*

To further characterize the codon optimized TDP-43 mediated effect, we used several wing and bristle drivers to overexpress TDP-43. The codon optimized TDP-43 misexpressed using the wing specific driver *beadex*^{MS1096}-GAL4 (*bx*^{MS1096}-GAL4) leads to pharate adults (unable to eclose from the pupal case) with smaller, necrotic wings (**Figure 3.4 C**). Unlike the codon optimized TDP-43 transgenic lines, the human wild-type TDP-43 misexpressed using *bx*^{MS1096}-GAL4 leads to viable adults, but with crumpled wings (**Figure 3.4 B**). The *scabrous*-GAL4 (*sca*-GAL4) driver is expressed in sensory organ precursors and in wing disc through late larval and pupal stages. Previously, we have used this driver to misexpress fly DVAP33, a gene linked to ALS8, that showed a loss of notal macrochaetae (Ratnaparkhi et al., 2008). Unlike the previous model, both human wild-type TDP-43 and codon optimized TDP-43 misexpression had no effect on macrochaetae, but the codon optimized wild-type TDP-43 produced

pharate adults with necrotic wings that are unable to expand (**Figure 3.4 F**). Vanden Broeck et al. previously showed that both up and downregulation of the fly dTDP-43 cause selective apoptosis in the crustacean cardioactive peptide (CCAP)/bursicon neurons (Vanden Broeck et al., 2013). Loss of CCAP/bursicon neurons have been shown to cause pupal lethality with escapers that show wing expansion defect phenotypes (Park et al., 2003). Upon expression of wild-type TDP-43 in the CCAP/bursicon neurons using CCAP-GAL4, we observed a similar wing expansion defect in 1 day post-eclosion adults (**Figure 3.3 H**). Misexpression of codon-optimized TDP-43 in CCAP/bursicon neurons showed smaller, necrotic and swollen wings compared to control flies (**Figure 3.4 I**). Since we failed to see an effect of TDP-43 on macrochaetae using *sca*-GAL4, we used another bristle specific driver *equator*-GAL4 (*eq*-GAL4) to misexpress human and codon optimized wild-type TDP-43 in the *Drosophila notum*. Both control and human wild-type TDP-43 flies show normal macrochaetae formation (**Figure 3.4 J and K**). However, codon optimized TDP-43 shows a dramatic loss in notal macrochaetae (**Figure 3.4 L, white arrows**). Moreover, the bristles present exhibit the *singed* phenotype that is marked by the thinning and curling of the bristles towards the tip (**Figure 3.4 L, black arrows**). These results suggest that misexpression of codon optimized wild-type TDP-43 transgenic fly causes smaller wings with abnormal morphology and bristle irregularities in the *Drosophila notum*.

Misexpression of codon optimized TDP-43 mimic cellular and molecular phenotypes seen in pathological disease state

Since we observed a more robust phenotype with the codon optimized wild-type TDP-43, we wanted to investigate the protein levels in these flies. Using the various *glass* direct promoter fusion lines and the SevEP-GAL4 driver, we overexpressed TDP-43 in the fly eye and evaluated total protein level by immunoblotting. Compared to the GMR-GAL4 driven human TDP-43 transgenic flies, the codon optimized flies express more monomeric total TDP-43 protein in multiple *gl*-TDP-43 lines (**Figure 3.5 A, lane 5, 6 and 7**). Of these, the *gl*-TDP-43^{CO3} was previously used to demonstrate the robust eye phenotype and it is also the line that was used in the subsequent experiments. Unlike the *gl*-TDP43 lines, the SevEP-GAL4 driven codon optimized line did not show an increase in total TDP-43 expression, which is expected since it is only expressed in a subset of photoreceptor neurons (**Figure 3.5 A, lane 8**). We used the *gl*-TDP-43^{CO3} line and the stable recombinant Sev-EP-GAL4, UAS-TDP-43^{CO} line to further investigate the expression of higher molecular weight species of TDP-43. We were able to detect higher molecular weight species of TDP-43 in SDS-PAGE under non-denaturing conditions in the codon-optimized lines, specifically *gl*-TDP-43^{CO3}. Along with the detection of higher molecular weight species, which is absent in human TDP-43 flies, we also observed the 35 kD and 15 kD truncated fragments in the codon optimized flies that are claimed to be the toxic component of the TDP-43 aggregates (**Figure 3.5 B**).

We wanted to further investigate the localization of the protein in the neuronal cells. In third instar larvae imaginal eye disc, we co-stained with TDP-43 and a neuronal nuclear marker Elav and observed both nuclear and cytoplasmic expression of TDP-43 in all the lines. However, the codon optimized flies show presence of more protein and the *gl*-TDP-43^{CO3} flies show a more robust mislocalization of TDP-43 in the cytoplasm along with cytoplasmic aggregates (**Figure 3.6 C, white arrows**). The mislocalization of TDP-43 to the cytoplasm is easier to visualize in the posterior view of the eye disc, which was analyzed using methods previously described (**Figure 3.6 E-H**). Our observations led us to determine that TDP-43 has the propensity to form toxic protein aggregates when too much protein is present via a gain of function mechanism.

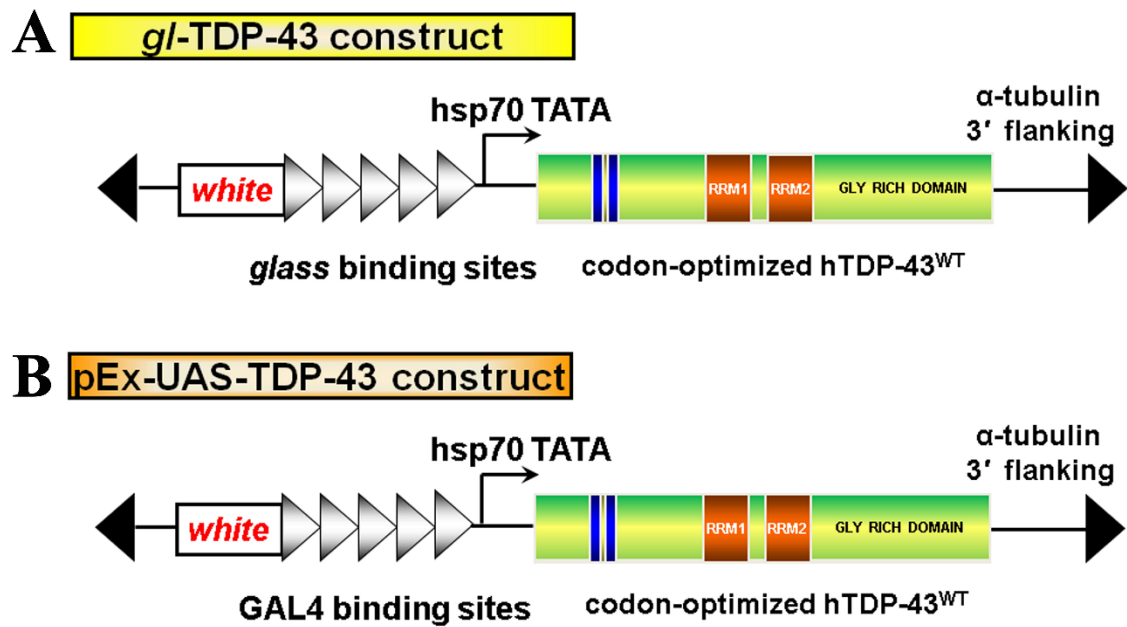
3.3 Conclusions

In order to better understand the pathogenic mechanism, many animal models have been generated in both vertebrate and invertebrate models of TDP-43. These animal models include deletions, RNAi mediated suppression, loss of function and gain of function models. Although the majority of the cases of ALS and FTLD-U are sporadic and involve non-mutant, wild-type TDP-43 mediated neurodegeneration, many of these models study the dominant disease specific mutants. The predominance of sporadic cases in these diseases therefore makes it important to better understand the mechanism of wild-type TDP-43 related pathogenesis that is independent of any dominant mutations. There have been some reports, both in sporadic and familial cases of FTLD-U, that there is

an increased expression of TDP-43 in patient brains. There is a possibility that TDP-43 has a dose-dependent effect on its propensity to form toxic aggregates. We utilized *Drosophila melanogaster* as an animal model to create a codon optimized wild-type TDP-43 transgenic line that expresses an increased level of TDP-43 as it is optimized to have a better expression in the invertebrate model. Compared to previously characterized human wild-type TDP-43 transgenic lines, these codon optimized TDP-43 lines form toxic cytoplasmic aggregates that gives rise to very robust phenotype when expressed in the *Drosophila* retina, wing, and bristle. The codon optimized wild-type TDP-43 model mimics the disease pathology and is an ideal tool to investigate the mechanism of pathogenesis irrespective of the dominant mutants that are associated with familial cases.

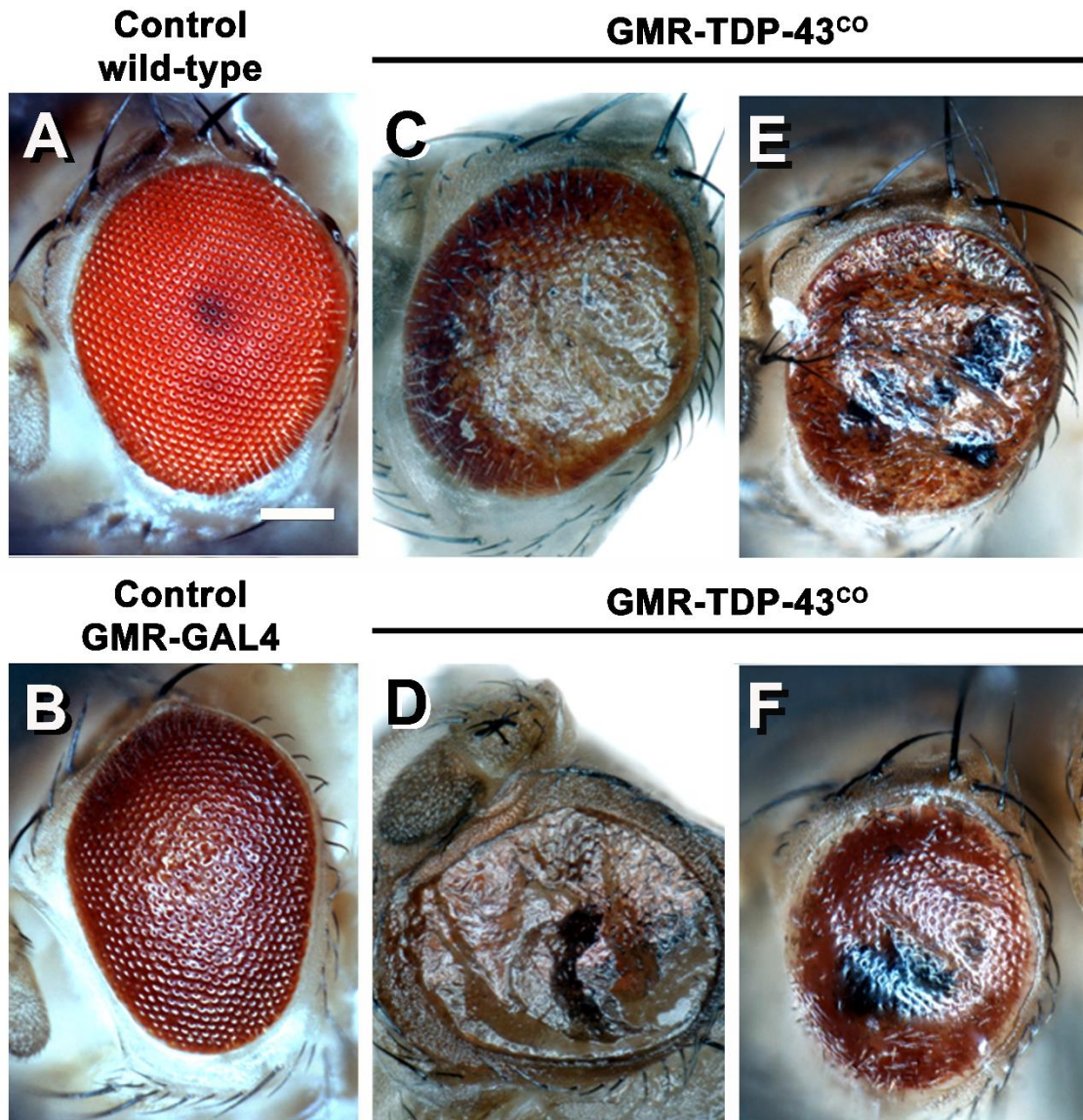
FIGURES

Figure 3.1. Schematic of codon optimized TDP-43 constructs



The codon-optimized TDP-43 constructs are used to create the transgenic codon optimized TDP-43 lines. The two types of lines generated use: **(A)** eye-specific *glass* direct fusion promoter vector and **(B)** UAS vector that requires a tissue specific GAL4 driver for TDP-43 expression.

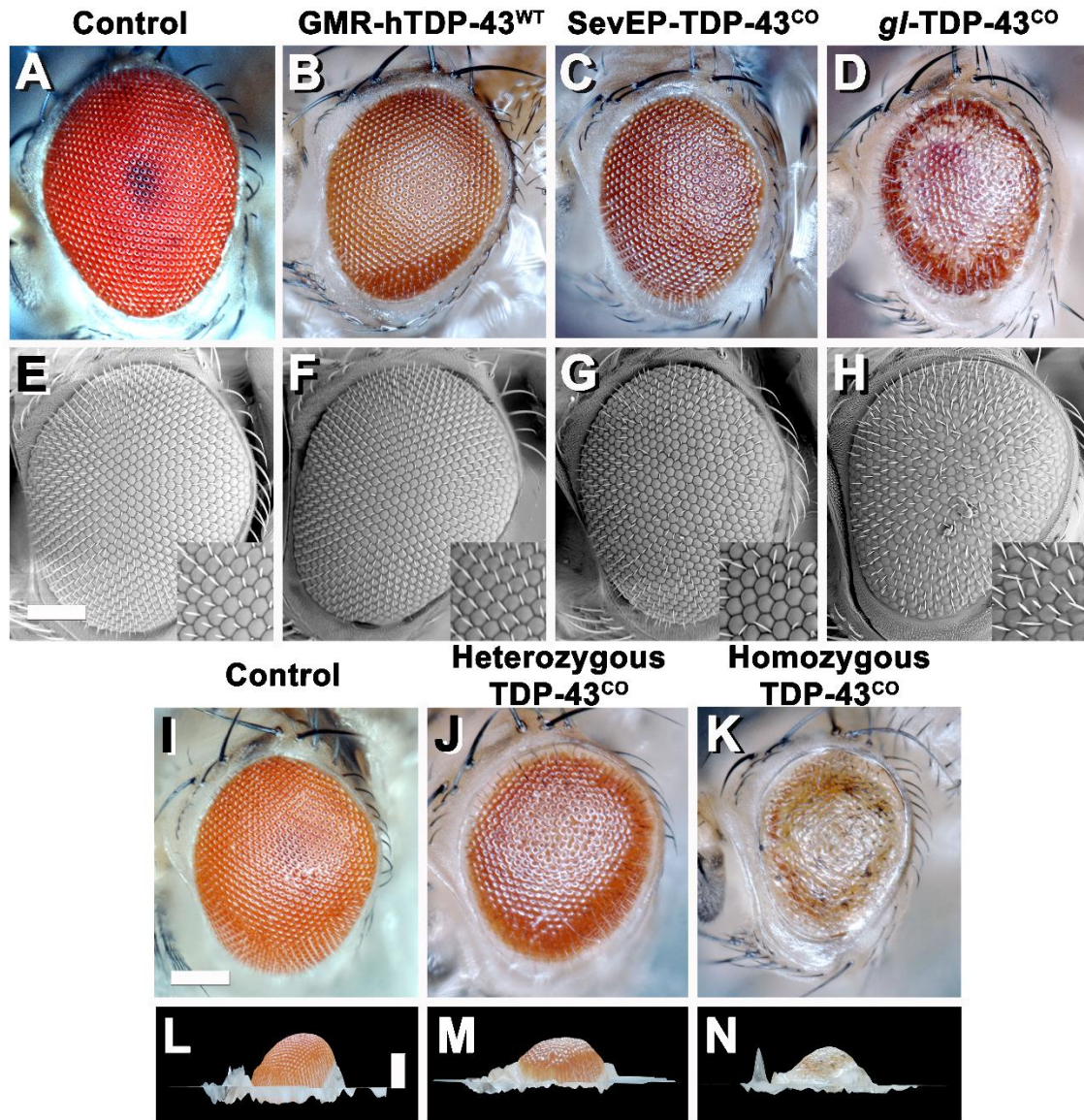
Figure 3.2. Misexpression of codon optimized TDP-43 using GMR-GAL4 driver induces robust phenotype in the external eye



All flies are grown at 18°C and images were taken 1 day post eclosion. **(A)** Control wild type eye. **(B)** Control promoter-only eye. **(C - F)** Escapers from 4 different lines of heterozygous codon optimized TDP-43 misexpression using eye-specific promoter (**C and D:** GMR-GAL4 on the X-chromosome and **E and F:**

GMR-GAL4 on the second chromosome). Upon TDP-43 misexpression, the eyes show severe depigmentation, irregularities in bristles, and necrotic patches or hypermelanization. Scale bar 50 μ M.

Figure 3.3. Misexpression of codon optimized TDP-43 induces depigmentation and irregularities in bristles as compared to existing human wild-type TDP-43 lines

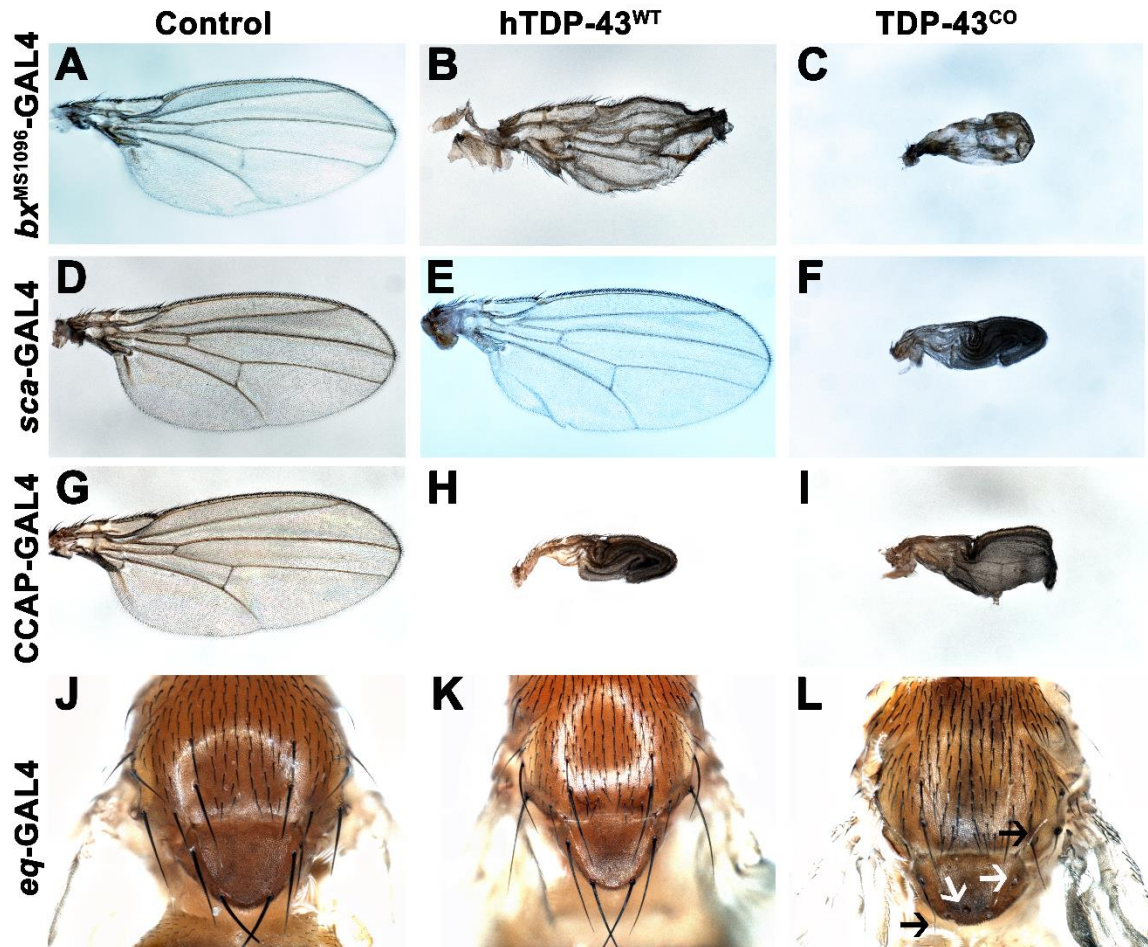


Transgenic flies stably express human wild-type TDP-43 and human codon optimized TDP-43 using eye promoters. All stocks were kept and maintained at room temperature (22°C). **(A-D)** Photomicrograph and **(E-H)** scanning electron

microscopy (SEM) images of the adult retina at 10 days post-eclosion (Scale bar 50 μ M). **(A and E)** Control wild-type Canton S fly. Compared to existing human wild-type TDP-43 transgenic flies **(B and F)**, the codon optimized wild-type TDP-43 flies exhibit a robust eye phenotype including depigmentation, disruption in the planar polarity and loss of bristles using both *glass* direct fusion promoter **(D and H)** and the milder GAL4 driver (SevEP-GAL4, a selective R3, R4 and R7 photoreceptor neuron driver) **(C and G)**. The robust phenotype mediated by codon optimized TDP-43 is both age and dose dependent **(I-N)**. At 1 day post-eclosion, codon optimized TDP-43 **(J)** shows less depigmentation compared to 10 days post-eclosion **(D)**. At 1 day post-eclosion, the homozygous codon optimized TDP-43 expression **(K)** shows a dramatically more robust phenotype with some necrosis compared to heterozygous codon optimized TDP-43 **(J)**. In addition, compared to wild-type Canton S flies **(I and L)**, both hetero- and homozygous codon optimized TDP-43 show decreased eye volume **(M and N respectively)**. Scale bar 100 nM.

Genotypes: **(A and E)** Canton S, **(B and F)** $w^{1118}/+;GMR-GAL4/+;UAS-hTDP-43^{WT}/+$, **(C and G)** $w^{1118}/+;SevEP-GAL4,UAS-TDP-43^{CO}/+;+$, **(D and H)** $w^{1118}/+;gl-TDP-43^{CO3}/+;+$, **(I and L)** Canton S, **(J and M)** $w^{1118}/+;gl-TDP-43^{CO3}/+;+$, **(K and N)** $w^{1118};gl-TDP-43^{CO3};+$.

Figure 3.4. Misexpression of codon optimized TDP-43 leads to wing expansion defects and swelling, as well as singed and loss of bristles in the *Drosophila notum*

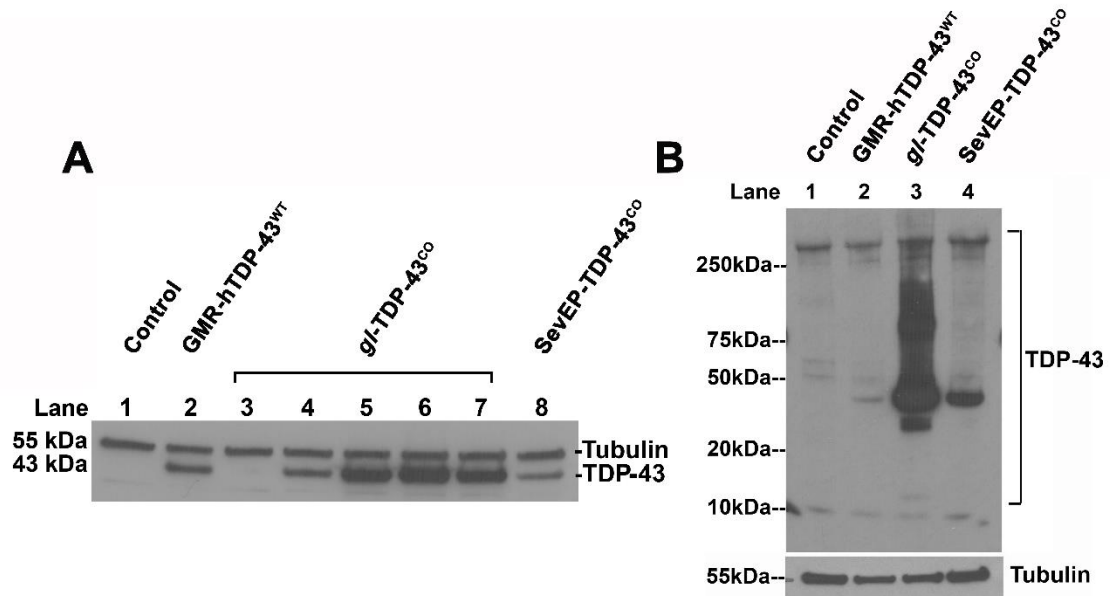


Misexpression of both codon optimized and non-codon optimized human TDP-43 in wings and bristles of transgenic flies. All crosses set and flies maintained at room temperature (22°C). **(A-C)** Codon optimized TDP-43 expressed in the wings using wing specific driver *bx^{MS1096}-GAL4* leads to pharate adults with smaller, swollen and necrotic wing **(C)**, as compared to healthy, viable adults expressing non-codon optimized human wild-type TDP-43 with crumpled wings

(B) and normal wings with driver alone **(A)**. **(D-F)** Using sensory neuron specific *sca*-GAL4 driver to drive the expression, non-codon optimized human wild-type TDP-43 flies **(E)** have normal wings, similar to driver alone **(D)**, but codon optimized TDP-43 causes pharate adults with smaller, necrotic wings with expansion defect **(F)**. **(G-I)** CCAP-GAL4, expressed in CCAP/ bursicon neurons in ventral nerve cord and subesophageal ganglion in the adult brain, driven expression of codon-optimized TDP-43 **(I)** as well as non-codon optimized human wild-type TDP-43 **(H)** also exhibits similar wing expansion defect phenotype, compared to driver alone **(G)**. **(J-L)** A bristle specific driver, *eq*-GAL4, causes a dramatic loss of bristles (white arrows) and *singed* bristles (black arrows) with codon optimized TDP-43 flies **(L)**, while non-codon optimized human wild-type TDP-43 **(K)** and driver alone **(J)** develop normal bristles.

Genotypes: **(A)** $w^{1118}, bx^{MS1096}\text{-GAL4/+;+;+}$, **(B)** $w^{1118}, bx^{MS1096}\text{-GAL4/+;+;+;UAS-hTDP-43}^{WT}/+$, **(C)** $w^{1118}, bx^{MS1096}\text{-GAL4/+;+;+;UAS-TDP-43}^{CO}/+$, **(D)** $w^{1118}/+; sca\text{-GAL4/+;+}$, **(E)** $w^{1118}/+; sca\text{-GAL4/+;+;UAS-hTDP-43}^{WT}/+$, **(F)** $w^{1118}/+; sca\text{-GAL4/+;+;UAS-TDP-43}^{CO}/+$, **(G)** $y^1, w^*/+; CCAP\text{-GAL4/+;+}$, **(H)** $y^1, w^*/+; CCAP\text{-GAL4/+;+;UAS-hTDP-43}^{WT}/+$, **(I)** $y^1, w^*/+; CCAP\text{-GAL4/+;+;UAS-TDP-43}^{CO}/+$, **(J)** $w^{1118}/+; eq\text{-GAL4/+;+;+}$, **(K)** $w^{1118}/+; eq\text{-GAL4/+;+;+;UAS-hTDP-43}^{WT}/+$, **(L)** $w^{1118}/+; eq\text{-GAL4/+;+;+;UAS-TDP-43}^{CO}/+$.

Figure 3.5. Codon-optimized TDP-43 transgenic fly expresses higher levels of protein

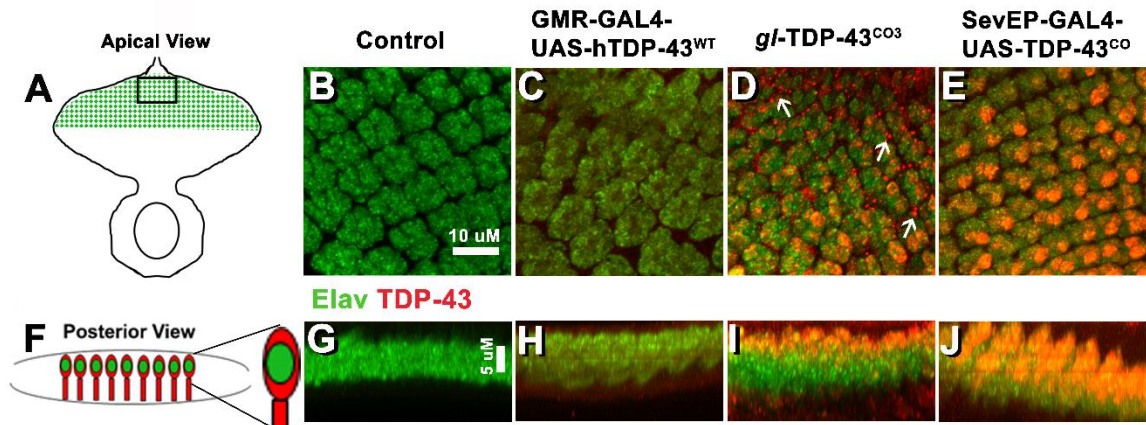


(A) Western blot analysis comparing the total TDP-43 levels in human wild-type TDP-43 (lane 2) to the different codon-optimized TDP-43 lines generated (lane 3-8) and wild-type Canton S flies (lane 1). All transgenic flies are expressing only one copy of the TDP-43 gene. Among the different codon-optimized TDP-43 lines, *gl*-TDP-43^{CO3}, *gl*-TDP-43^{CO4} and *gl*-TDP-43^{CO5} (lane 5, 6 and 7 respectively) have the highest expression, an almost 2-fold increase compared to non-codon optimized human wild-type TDP-43 (lane 2). Codon optimized TDP-43 expression driven with a milder driver, SevEP-GAL4, does not show increased expression of the total protein (lane 8). β -tubulin is presented as a loading control. **(B)** Codon optimized TDP-43 (*gl*-TDP-43^{CO3}, lane 3) exhibits higher molecular weight species of TDP-43, as well as the known 35 kD and 15 kD truncated fragments, compared to human wild-type TDP-43 (lane 2) or the

milder expression (SevEP-GAL4 driven) of codon optimized TDP-43 (lane 4). Lane 1 is wild-type Canton S control. β -tubulin is presented as a loading control.

Genotypes: **(A)** $w^{1118};+;+$, $w^{1118};\text{GMR-GAL4/+;UAS-hTDP-43}^{\text{WT}}/+$, $w^{1118};g/-\text{TDP-43}^{\text{CO1}}/+;+$, $w^{1118};+;g/-\text{TDP-43}^{\text{CO2}}/+$, $w^{1118};g/-\text{TDP-43}^{\text{CO3}}/+;+$, $w^{1118};g/-\text{TDP-43}^{\text{CO4}}/+;+$, $w^{1118};g/-\text{TDP-43}^{\text{CO5}}/+;+$, $w^{1118};\text{SevEP-GAL4,UAS-TDP-43}^{\text{CO}}/+;+$ (lane 1-8, respectively). **(B)** $w^{1118};+;+$, $w^{1118};\text{GMR-GAL4/+;UAS-hTDP-43}^{\text{WT}}/+$, $w^{1118};g/-\text{TDP-43}^{\text{CO3}}/+;+$, $w^{1118};\text{SevEP-GAL4,UAS-TDP-43}^{\text{CO}}/+;+$ (lane 1-4, respectively).

Figure 3.6. Codon-optimized TDP-43 transgenic flies show robust mislocalization of TDP-43 to the cytoplasm and form aggregates in larval eye discs



(A) is a schematic of the third instar larval eye imaginal disc (from the apical view); area in the rectangle is the area imaged. (B-E) Confocal images of the eye discs stained with neuronal nuclear marker Elav (green) and TDP-43 (red). There is a greater expression of both nuclear and cytoplasmic TDP-43 in codon optimized lines (D and E) as compared to human wild-type TDP-43 (C). The codon optimized flies exhibit a more robust mislocalization and aggregation of cytoplasmic TDP-43; white arrows in (D). (B) is wild-type Canton S as control (scale bar 10 μM). (F) is a schematic of the eye disc from the posterior view to better visualize the nuclear and cytoplasmic localization. (G-J) represents the posterior view of the eye discs to show nuclear and cytoplasmic TDP-43 expression. The area marked with green fluorescence is the nuclear region (Elav staining) and the surrounding area is cytoplasmic as illustrated by the schematic.

The codon optimized flies (**I and J**) show increased mislocalization of TDP-43 to the cytoplasm (Scale bar 5 μ M).

Genotypes: (**A and E**) Canton S, (**B and F**) $w^{1118};GMR-GAL4/+;UAS-hTDP-43^{WT}/+$, (**C and G**) $w^{1118};g/-TDP-43^{CO3}/+;+$, (**D and H**) $w^{1118};SevEP-GAL4,UAS-TDP-43^{CO}/+;+$.

Table 3.1. Summary of TDP-43 misexpression in the fly eye

Crosses at 25°C		
	GMR-GAL4 (X)	GMR-GAL4 (II)
UAS-TDP-43 ^{C01}	Lethal	Lethal
UAS-TDP-43 ^{C02}	Lethal	Lethal
UAS-TDP-43 ^{C03}	Lethal	Lethal
UAS-TDP-43 ^{C04}	Lethal	Lethal
UAS-TDP-43 ^{C05}	Lethal	Lethal
UAS-TDP-43 ^{C06}	Lethal	Lethal
UAS-TDP-43 ^{C07}	Survived; not a strong phenotype	Survived; not a strong phenotype
UAS-TDP-43 ^{C08}	Lethal	Lethal
Crosses at 18°C		
	GMR-GAL4 (X)	GMR-GAL4 (II)
UAS-TDP-43 ^{C01}	Lethal	Lethal
UAS-TDP-43 ^{C02}	Survived; depigmentation, unorganized bristles without planer polarity, loss of volume	Few escapers; depigmentation and necrotic patches
UAS-TDP-43 ^{C03}	Lethal	Lethal
UAS-TDP-43 ^{C04}	Lethal	Few escapers; depigmentation and necrotic patches
UAS-TDP-43 ^{C05}	Lethal	Lethal
UAS-TDP-43 ^{C06}	Lethal	Lethal
UAS-TDP-43 ^{C07}	Survived; not a strong phenotype	Survived; not a strong phenotype
UAS-TDP-43 ^{C08}	Survived; depigmentation, unorganized bristles without planer polarity, loss of volume	Lethal

Eight different lines of the codon optimized TDP-43 transgenic flies were generated using the UAS vector that allows for tissue specific expression. All the different UAS-TDP-43^{CO} lines generated were crossed to two different GMR-GAL4 lines. All of these transgenic flies only express one copy of the TDP-43 gene. The flies were maintained at two different temperature (18°C and 25°C). At a higher temperature, lethality was observed upon TDP-43 expression for most lines. At a lower temperature, lethality was observed only in a few lines. Some of the lines maintained at lower temperature produced escapers and stable progeny that all show robust eye phenotype.

CHAPTER IV: MISEXPRESSION OF TDP-43 AND AUTOPHAGY

4.1 Introduction

Autophagy in neurodegeneration

One of the hallmarks of neurodegenerative diseases is the presence of misfolded protein aggregates. These aggregates trigger cellular stress and cells have an innate mechanism to clear such toxic aggregates. Autophagy is a cellular process by which cytosolic components, including protein aggregates, are engulfed into a multimembrane vesicle and fused with the endosomal/lysosomal compartments to be degraded (Kundu and Thompson, 2008; Lamark and Johansen, 2012; Mizushima, 2007). Autophagy was first described by Ashford and Porter in rat liver cells when these cells were treated with glucagon (Ashford and Porter, 1962). There are many known functions of autophagy in eukaryotic cells in addition to clearing toxic aggregates. Autophagy plays a role in embryonic development and in post-development cellular differentiation (Mizushima and Levine, 2010). In mature cells, autophagy is vital for maintenance of cellular homeostasis and quality control (Kundu and Thompson, 2008; Mizushima, 2007). In *Drosophila*, autophagy takes place in larval fat bodies and salivary glands. Additionally, the ubiquitin proteasomal system (UPS) provides another cellular mechanism for misfolded protein degradation. A disruption in the autophagy process or the proteasomal system can lead to cellular imbalance and has been linked to many neurodegenerative diseases, such as Alzheimer's disease, Parkinson's disease, Huntington's

disease and ALS (Lamark and Johansen, 2012; Pandey et al., 2007; Wong and Cuervo, 2010). In patients with Alzheimer's disease, autophagic vacuoles, including autophagosomes, multivesicular bodies (MVB) and lysosomes, accumulate (Filimonenko et al., 2007). In addition, many animal models of neurodegeneration also show autophagic dysfunction. In mice models with presenilin mutation, a protein involved in Alzheimer's disease pathology, as well as Parkinson's disease models, it has been shown that dysfunction of the lysosomal proteasome system and accumulation of autophagic vacuoles contributes to the pathology (Lee et al., 2010). These phenotypes are also observed in ALS mice models of SOD1 (Morimoto et al., 2007). It has been well established that autophagic dysfunction is a major player involved in toxic protein mediated neurodegeneration (Wong and Cuervo, 2010).

Autophagy signaling and machinery

There are three types of autophagy: chaperone-mediated autophagy, microautophagy, and macroautophagy (Mizushima, 2007). Chaperone-mediated autophagy, mostly seen in higher eukaryotes, requires the cytosolic protein to bind to cytosolic chaperones and integrate with the lysosome through lysosomal-associated membrane protein (LAMP-2) (Kundu and Thompson, 2008). In microautophagy, lysosomal membranes engulf cytosolic components and form new smaller vesicles within the acidic lumen to carry out the degradation process (Lamark and Johansen, 2012; Mizushima, 2007). The most predominant form of autophagy is macroautophagy, which requires a newly synthesized double

membrane to form a vesicle known as autophagosome. Autophagosomes then fuse with lysosomes or with late endosomes to form autolysosomes or amphisomes, respectively (Kundu and Thompson, 2008). Autophagy requires three major steps: induction of autophagy, formation of the autophagosome and degradation. In the induction step, the isolation membrane is formed and involves key autophagic genes that translate autophagy-related proteins (Atg) such as Atg8 (LC3) and Atg5. The next step is for the membrane to engulf the cytosolic components that are going to be degraded and form a double membrane, giving rise to the autophagosome, where Atg5 is still present. The last step is for the autophagosome to fuse with acidic lysosomes to form the autolysosome, which is recognized by the presence of Atg8 (Kundu and Thompson, 2008; Lamark and Johansen, 2012; Mizushima, 2007; Ravikumar et al., 2010; Scott et al., 2007; Yang and Klionsky, 2010).

Autophagy is typically inhibited by target of rapamycin when ample nutrients are present. Target of rapamycin (TOR), a serine/threonine kinase involved in cell growth, cell proliferation, cell survival and protein synthesis, is known to inhibit Atg1, a kinase involved in autophagosome formation earlier in the process (Neufeld, 2010; Scott et al., 2007). The involvement of autophagic dysfunction in neurodegeneration has recently been a major focus for understanding disease mechanisms. Under nutrient depletion, starving conditions, TOR no longer inhibits Atg1 and autophagy mediated clearance can take place. In addition to bulk degradation of the cytosolic components by

autophagy, a more selective form of autophagy is also present that can occur in mitochondria, also known as mitophagy, and peroxisomes (Nair and Klionsky, 2005). Selective autophagy requires adapter molecules, such as p62/sequestosome 1 (SQSTM1) (Pankiv et al., 2007) or ALFY (Filimonenko et al., 2010). The fly homologue of ALFY is known as blue cheese and is known to be involved in a more selective autophagy rather than starvation induced autophagy (Finley et al., 2003).

Autophagy in TDP-43 proteinopathies

As mentioned before, autophagy has been suggested to be involved in many neurodegenerative diseases, including ALS (Wong and Cuervo, 2010). In patients with sporadic ALS, accumulation of autophagosomes was observed in the spinal cord (Sasaki, 2011). Since the initial observation in these patients, many have looked into the role of autophagy in animal models. The neurodegenerative pathology involving autophagic dysfunction is well documented. Full length and c-terminal fragments of TDP-43 have also been shown to induce mitochondrial specific autophagy or mitophagy (Temiz et al., 2009). Oddo and colleagues reported that the toxic c-terminal TDP-43 fragment accumulation increases when autophagy is inhibited and the inhibition of mTOR by rapamycin rescues the phenotype (Caccamo et al., 2009). Rapamycin has also been shown to slow down motor dysfunction and rescue learning and memory impairment in a mouse model of TDP-43 (Wang et al., 2012).

Additionally, others have shown that autophagy inhibition by 3-methyladenine blocked degradation of wild type and mutant TDP-43 mutually by the ubiquitin proteosomal system (UPS) and autophagic degradation mechanisms (Wang et al., 2010). Hu and colleagues were one of the first groups to report that TDP-43 aggregates colocalize with autophagic markers and is downregulated when p62/SQSTM1 is overexpressed (Brady et al., 2011). Since then, there have been reports that link TDP-43 downregulation along with loss of Atg7, leads to an impairment of autophagy and accumulation of p62, suggesting that TDP-43 plays a role in the regulation of autophagy (Tashiro et al., 2012). Recently, Shaw and colleagues reported that soluble TDP-43 is degraded by UPS, while larger aggregates require autophagy for clearance (Scotter et al., 2014). The role of autophagy in TDP-43 mediated neurodegeneration is still unclear. Further investigations on how the autophagy mechanism regulates these large aggregates and the role TDP-43 plays in activating autophagy are needed.

4.2 Results

Morphological and functional disruption of the photoreceptor neurons upon TDP-43 misexpression

In other *Drosophila* models of neurodegenerative disease that study the retina, such as Huntington's disease, it has been found that expressing toxic proteins in the eye causes an alteration in the photoreceptor neurons (Jackson et al., 1998). As mentioned before, the robust external eye phenotype led us to

hypothesize that the internal structures of the eye might also be affected by TDP-43 misexpression. Therefore, the next logical step was to look at the internal morphology of the photoreceptor cells. One of the advantages of using a *Drosophila* model is that there are many easy techniques available that allow one to look at the inner structures of the eye. With a light microscope we can visualize the photoreceptor cells using a technique called optical neutralization. This technique allows the cornea of the eye to be neutralized using immersion oil, which has the same refractive index as the cornea. The neutralization permits easy visualization of the inner structures of the rhabdomere. Upon codon optimized TDP-43 misexpression in the eye, the photoreceptor cells exhibit an altered morphology, where they appear to be more flat compared to wild type controls (**Figure 4.1 C, yellow arrows**). This means that TDP-43 misexpression is affecting the photoreceptor neurons in the eye.

To investigate further, we utilized the *glass* direct fusion line and observed the degenerative phenotype in as early as 1 day post-eclosion flies expressing codon optimized TDP-43. Adult eyes were stained with fluorescent phalloidin, which stains the F-actin in cells and TDP-43 antibody. The *gl*-TDP-43^{CO3} flies exhibit an altered morphology of the photoreceptor neurons, which appear to be flattened and have a disruption in rhabdomere separation (**Figure 4.1 I, white arrows**) when visualized in tangential view of the adult retina. TDP-43 did not co-localize with the rhabdomere structures, but seems to be expressed in eye. To further characterize this phenotype, we also looked at the longitudinal view of the

adult retina. Most notably, the retina thickness is lessened and the rhabdomere length is shorter in *gl*-TDP-43^{CO3} flies. Along with Phalloidin, the retina was also stained with Elav, a neuronal nuclear marker, and TDP-43 antibody. Similar to what was observed in the larval eye imaginal discs (refer to chapter III), the localization of TDP-43 is observed in the nucleus and cytoplasm of these photoreceptor cells. Upon codon-optimized TDP-43 misexpression, there is a disruption in the normal length and morphology of these photoreceptor neurons as well as the presence of large vacuolar structures (**Figure 4.2 F-I, white arrow heads**).

These morphological disruptions led us to look further into the physiological effect of these photoreceptor neurons due to TDP-43 misexpression. Using extracellular electroretinogram (ERG) recordings that measure the response of photoreceptors to a light stimulus, we looked at the effects of TDP-43 misexpression, compared to both wild-type Canton S and GMR overexpressing RFP controls (**Figure 4.2 J-L**). At 1 day post-eclosion, the *gl*-TDP-43^{CO3} flies show a reduction in both the amplitude of ERG on transient (n=15 and p<0.01 compared to Canton S and p<0.01 compared to GMR-RFP) and depolarization (n=15 and p<0.01 compared to Canton S and p<0.01 compared to GMR-RFP) compared to controls (**Figure 4.2 M and N**). Taken together, these results suggest that codon optimized wild-type TDP-43 misexpression causes structural and functional degenerative phenotypes in the adult retina.

TDP-43 misexpression induced vacuoles are similar to autophagic intermediates

The presence of large vacuolar structures in the adult retina was a distinctive feature of the misexpression of codon optimized TDP-43. Recently, autophagy has been implicated to be involved in many neurodegenerative diseases, including ALS. We wanted to see if these vacuoles could possibly be a representation of autophagic intermediates. We used a live imaging technique in larval eye discs using LysoTracker, a detector of lysosomes or other acidic organelles that are indicative of induction of autophagy. Upon TDP-43 misexpression, we detected more acidic punctae compared to control and these acidic vacuoles are more elongated and larger in size compared to control (**Figure 4.3 C, white arrows and 4.3 D**).

One of the characteristics of neurodegenerative disease is the accumulation of misfolded protein aggregates and autophagy is one of the cellular process that degrades these unwanted protein aggregates. Jackson and colleagues reported tau induced autophagy and found accumulation of larger autophagic intermediates termed giant autophagic bodies (GAB). GABs are typically larger and less acidic than most intermediates or autophagosomes (Bakhoum et al., 2014). Similar to the previous observations with tau misexpression, TDP-43 misexpression also leads to the presence of vacuoles that are indicative of autophagic intermediates. Whether or not these vacuoles are similar to GABs remains to be determined. As previously observed, we

wished to characterize the large vacuoles that we observed in the adult retina. Using a GMR-GAL4 driver *in trans* to the *gl*-TDP-43^{CO3} line, we coexpressed codon optimized TDP-43 and a key autophagy protein, Atg5, that is responsible for the formation of the autophagosomes. We found that these large vacuoles in the adult retina were positive for Atg5 and it co-localized with TDP-43 (**Figure 4.4 B-E**).

Mature autolysosomes are known to be acidified and we wanted to determine the relative acidity of the lysosomes that we had observed in the imaginal eye disc. We used a genetic marker, Atg8-mCherry-GFP, which is a tandem reporter. Expression of this gene allows the detection of Atg8, a autophagic protein that is localized in autophagic intermediates, using the mCherry signal. In addition, a pH sensitive GFP is tagged to the Atg8 gene. This pH sensitive GFP only emits signal at a neutral pH. Upon coexpression of *gl*-TDP-43^{CO3} with this genetic marker, we found that of all the punctate positive for Atg8 mCherry, only a subset of the relative smaller punctae were also stained with GFP, indicating non-acidic compartments (**Figure 4.4 G-I, arrow heads**). Majority of the punctae, which were larger in size, were only fluorescent for Atg8 mCherry (**Figure 4.4 G-I, white arrows**), indicating more acidic mature autolysosomes. From these observations, we concluded that misexpression of codon optimized TDP-43 leads to increased acidic lysosomal vacuoles positive for autophagy markers.

TDP-43 misexpression changes the levels of proteins involved in mTOR signaling

Autophagy is known to be regulated by the mTOR signaling pathway. The large vacuolar structures that were positive for autophagy markers noticed in TDP-43 misexpressed flies seem similar to autophagic intermediates. To further conclude whether autophagy plays a role in TDP-43 mediated degeneration or not, we examined the levels of key proteins known to be involved in the mTOR signaling pathway. Using Western blot analysis, the levels of phosphorylated p70S6K, phosphorylated 4E-BP and phosphorylated AKT proteins were identified. Both phospho-p70S6K and phospho-4E-BP levels increased when TDP-43 is misexpressed (**Figure 4.5 A and B**). Both of these phosphorylated proteins are involved in the mTOR signaling pathway that controls an autophagic balance within the cell. Upon quantification of these blots (n=4), we found that the increase in phospho-p70S6K was not statistically significant ($p>0.05$, **Figure 4.5 D**), but the increased level of phospho-4E-BP was statistically significant ($p\leq 0.02$, **Figure 4.5 E**). The increased level of phosphorylated p70S6K at specific Thr 398 site and phosphorylation of 4E-BP at Thr 37/46 sites are both indicative of pro-growth regulation and inhibition of the induction of autophagy through the mTORC1 pathway. However, the role of p70S6K has previously been shown to induce autophagy in *Drosophila* independent of TOR signaling (Scott et al., 2004).

The levels of phospho-AKT decreases upon TDP-43 misexpression (**Figure 4.5 C**), but only for one of the isomers of AKT which is statistically significant ($p \leq 0.001$, **Figure 4.5 F**). The specific phosphorylation of Ser 505 site is known to be regulated by mTORC2. A decrease in the level of this phosphorylation may indicate that AKT is not regulated by the mTORC2. The mTORC2 mediated phosphorylation of AKT and other substrates has been linked to cell survival, metabolic regulation and cytoskeleton organization. The results observed here are preliminary and require further investigations. While these results seem contradictory to what we observed in the adult retina immunostaining, we cannot conclusively assume that changes in the mTOR signaling pathway are responsible for the increased lysosomal-autophagic vacuoles. It is also possible that autophagy is not being activated by the mTOR signaling pathway. Whether TDP-43 induced toxicity is mediated through this signaling pathway remains to be determined.

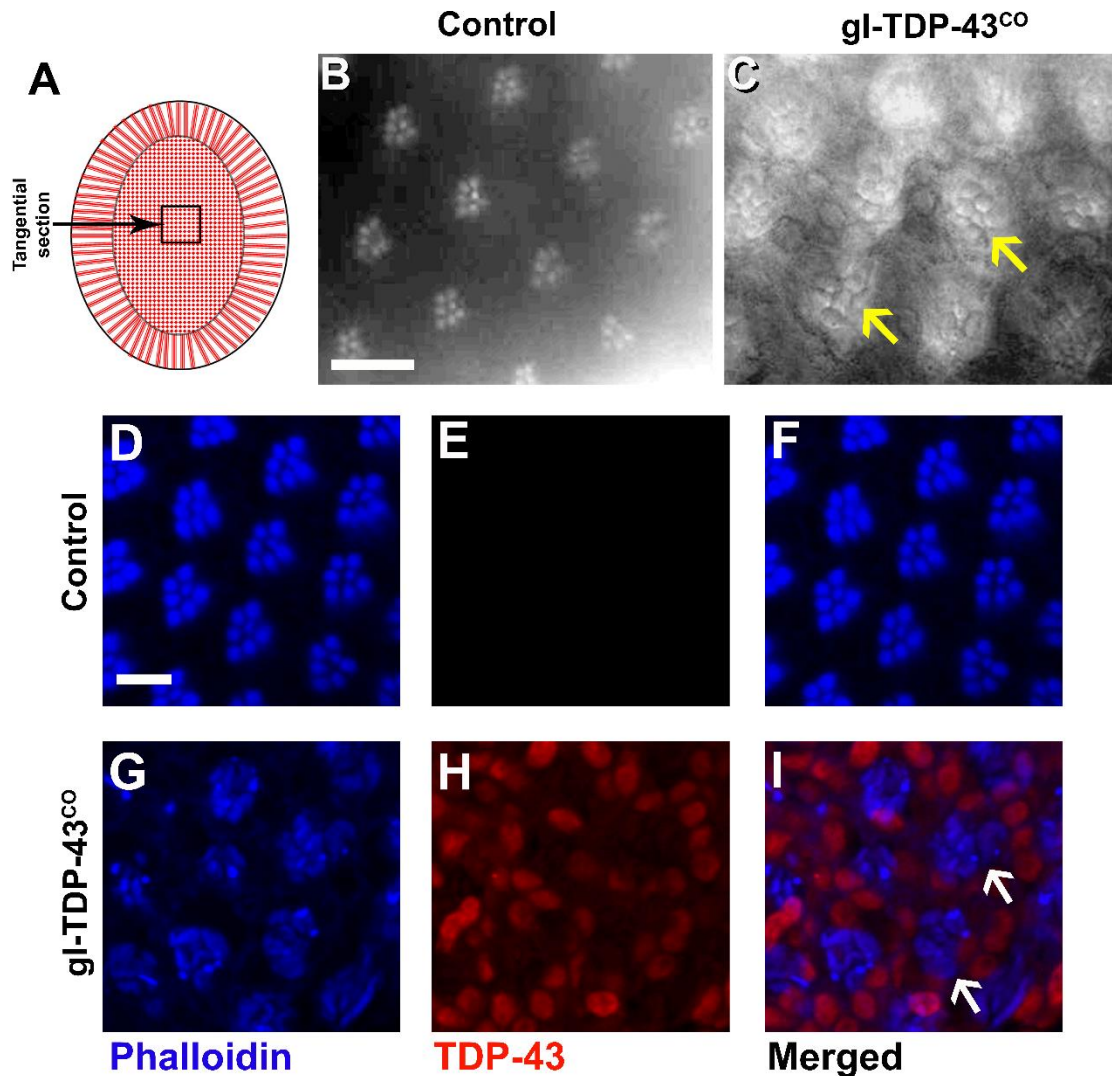
4.3 Conclusions

Further characterization of the retinal phenotype revealed a disruption in the morphology and function of the photoreceptor neurons, as well as presence of acidic autophagic/lysosomal vacuoles that are positive for key autophagy proteins. Current literature, along with the results reported here, indicates that autophagic dysfunction might play a role in TDP-43 mediated neurodegeneration. To date, the exact role of autophagy in TDP-43 proteinopathies is not well understood. The codon optimized TDP-43 misexpression model in the

Drosophila eye is an ideal *in vivo* system to study the possible role of autophagic dysfunction in TDP-43 proteinopathies. The involvement of autophagy in TDP-43 proteinopathies could unveil the underlying mechanism of TDP-43 mediated neurodegeneration and eventually aid in the identification of potential therapeutic targets.

FIGURES

Figure 4.1. TDP-43 misexpression causes altered morphology of the photoreceptor neurons in adult retina

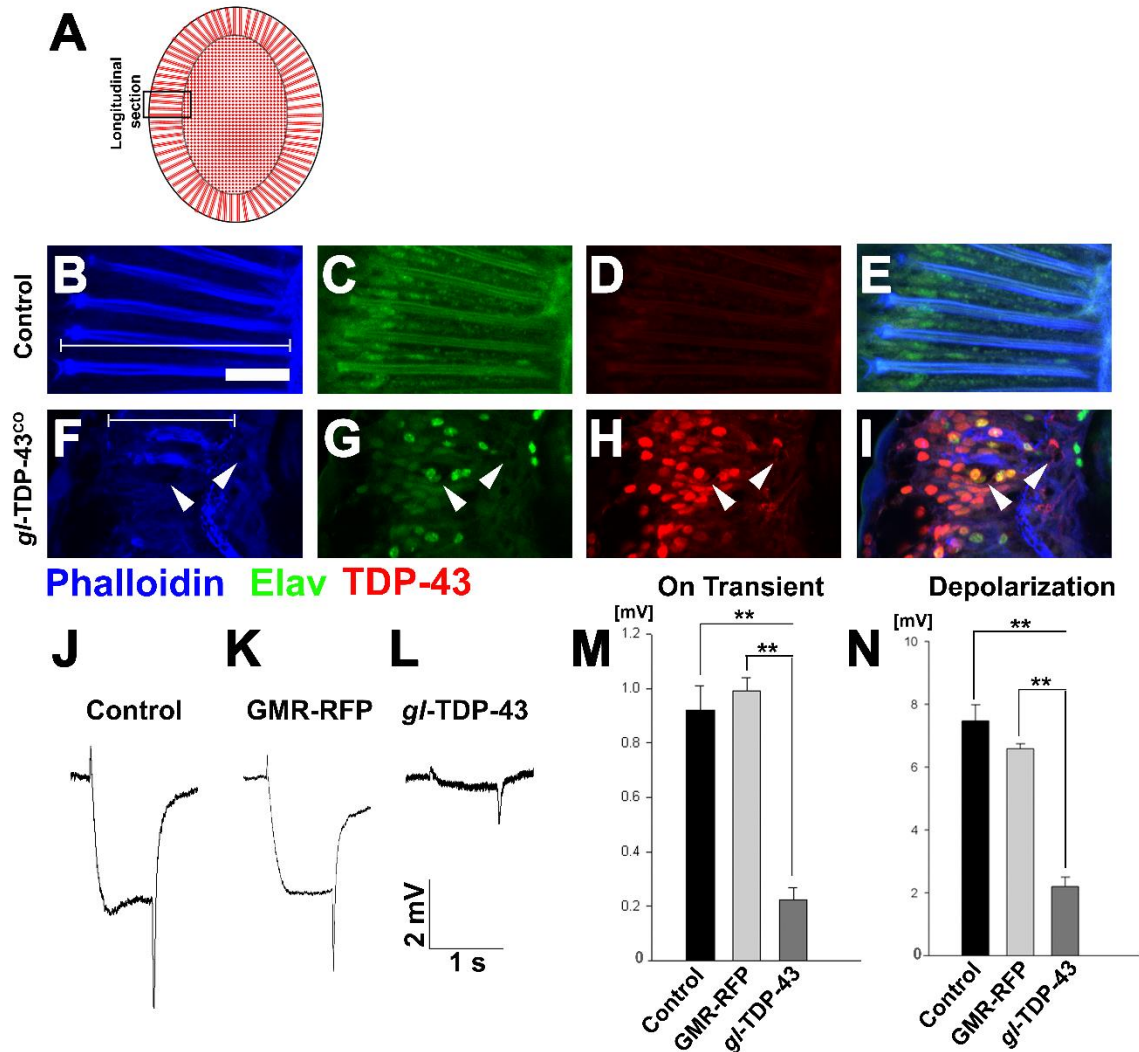


(A) represents a schematic of the adult eye and the area inside the rectangle is where the images were obtained. Optical neutralization of the 1 day post eclosion adult retina reveals that codon optimized TDP-43 flies (C) have altered rhabdomere morphology compared to control wild type Canton S flies (B). Scale bar 5 μ M. Similarly, immunostaining of the adult eye with phalloidin (F-actin

marker) showed that the codon optimized TDP-43 flies **(G-I)** exhibit rhabdomere separation defect and flattened structures of the rhabdomeres (white arrows) in 1 day post-eclosion adult compared to control **(D-F)**. These images represent the tangential view of the adult retina (scale bar 5 μ M).

Genotypes: **(A, C-E)** wild type Canton S, **(B, F-H)** $w^{1118}/+;g/-TDP-43^{CO3}/+;+$.

Figure 4.2. TDP-43 misexpression causes degeneration and functional disruption of the photoreceptor neurons in the adult retina

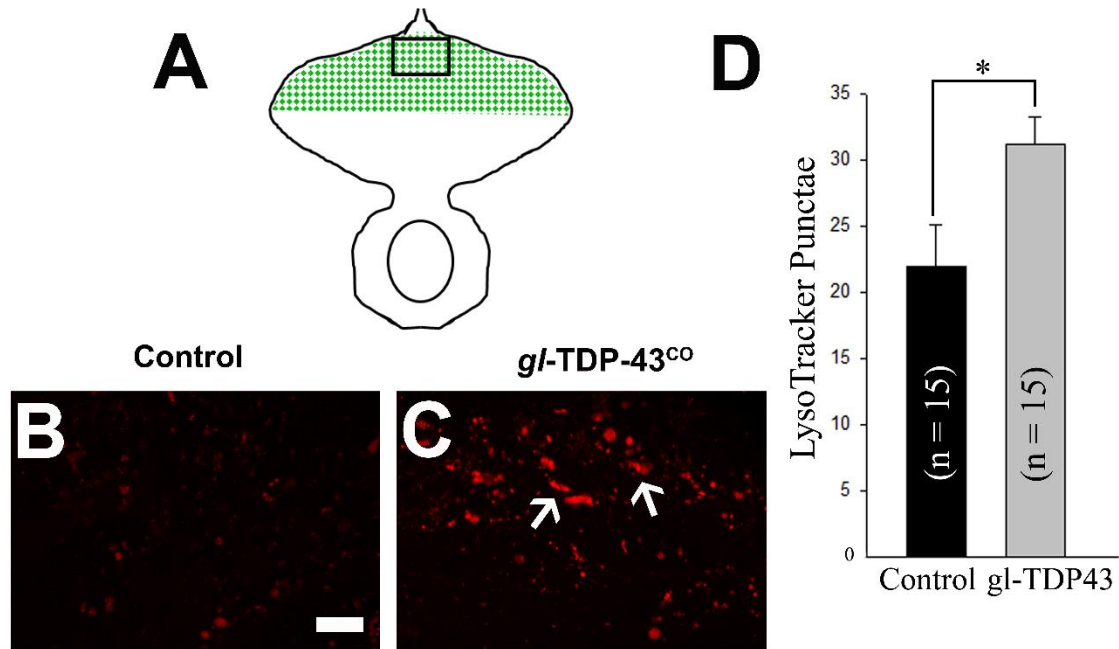


(A) represents a schematic of the adult eye and the area inside the rectangle is where the images were obtained. **(B-I)** are confocal images of the longitudinal view of the adult retina. The codon optimized TDP-43 flies **(F-I)** show altered photoreceptor morphology that appears to be shorter compared to wild type control **(B-E)**. The codon-optimized TDP-43 flies contain large vacuoles (white arrow heads) in 1 day post-eclosion adult retina (scale bar 10 μ M). **(J-L)** The

ERG traces of wild-type Canton S control, promoter driving RFP control and codon optimized TDP-43 in 1 day post-eclosion adults, respectively. Quantification of the ERG response amplitude for on transient **(M)** and depolarization **(N)**, along with the traces, show that codon optimized TDP-43 flies have decreased response for both. For on transient effect, n=15 and p-value between both groups is $p < 0.01$ **(M)**, and for depolarization effect, n=15 and the p-value between both groups is $p < 0.01$ **(N)**. The statistical analysis was performed using one-way ANOVA with Bonferroni's correction.

Genotypes: **(A-D)** wild type Canton S, **(E-H)** $w^{1118}/+;g/-TDP-43^{CO3}/+;+$, **(I)** wild type Canton S, **(J)** $w^{1118},GMR-myr-mRFP$, **(K)** $w^{1118}/+;g/-TDP-43^{CO3}/+;+$.

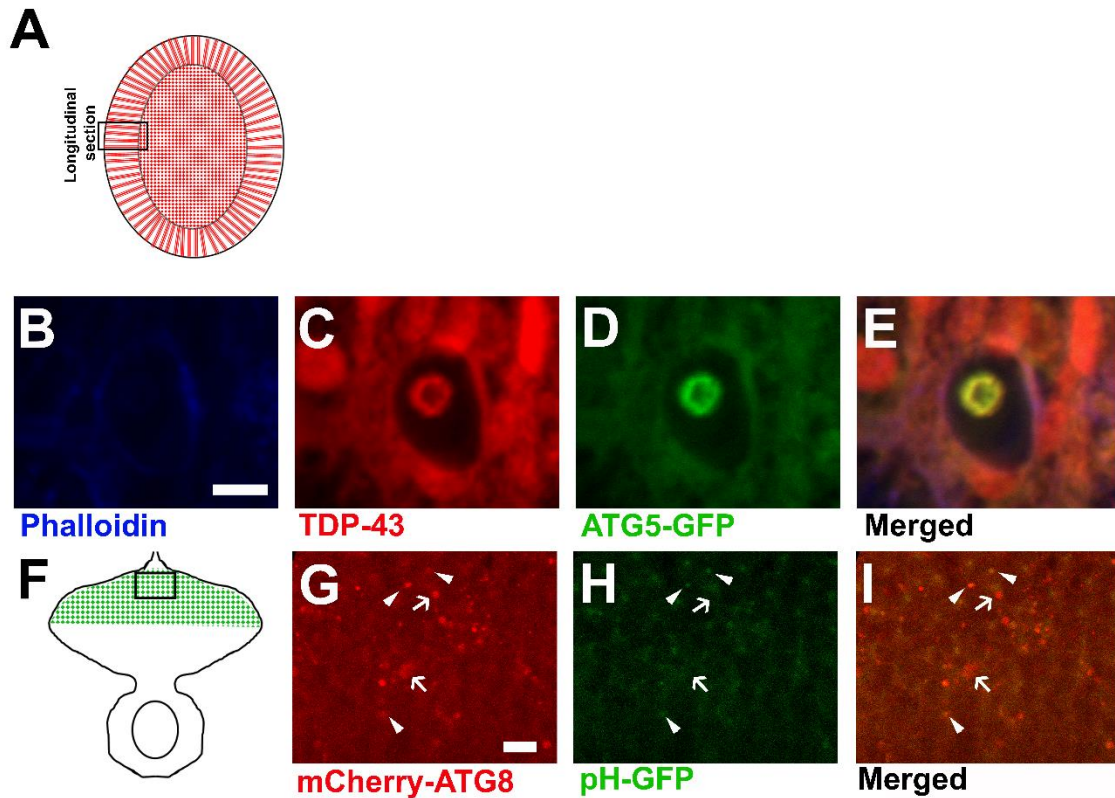
Figure 4.3. TDP-43 misexpression leads to an increase in lysosomal vacuoles



(A) represents the schematic of the third instar larval eye imaginal disc and the area in rectangle is the area imaged. Live staining of the third instar imaginal eye discs with LysoTracker dye shows an increase in lysosomal puncta in codon optimized TDP-43 flies (C) compared to wild-type Canton S control (B). Scale bar 10 μ M. (D) shows quantification of (B and C), n=15. For statistical significance, paired Student's t-test with two-tailed distribution of equal variance was performed (p=0.02).

Genotypes: (A) wild-type Canton S, (B) $w^{1118}/+; gl-TDP-43^{CO3}/+; +$.

Figure 4.4. TDP-43 misexpression induced vacuoles are positive for autophagy markers

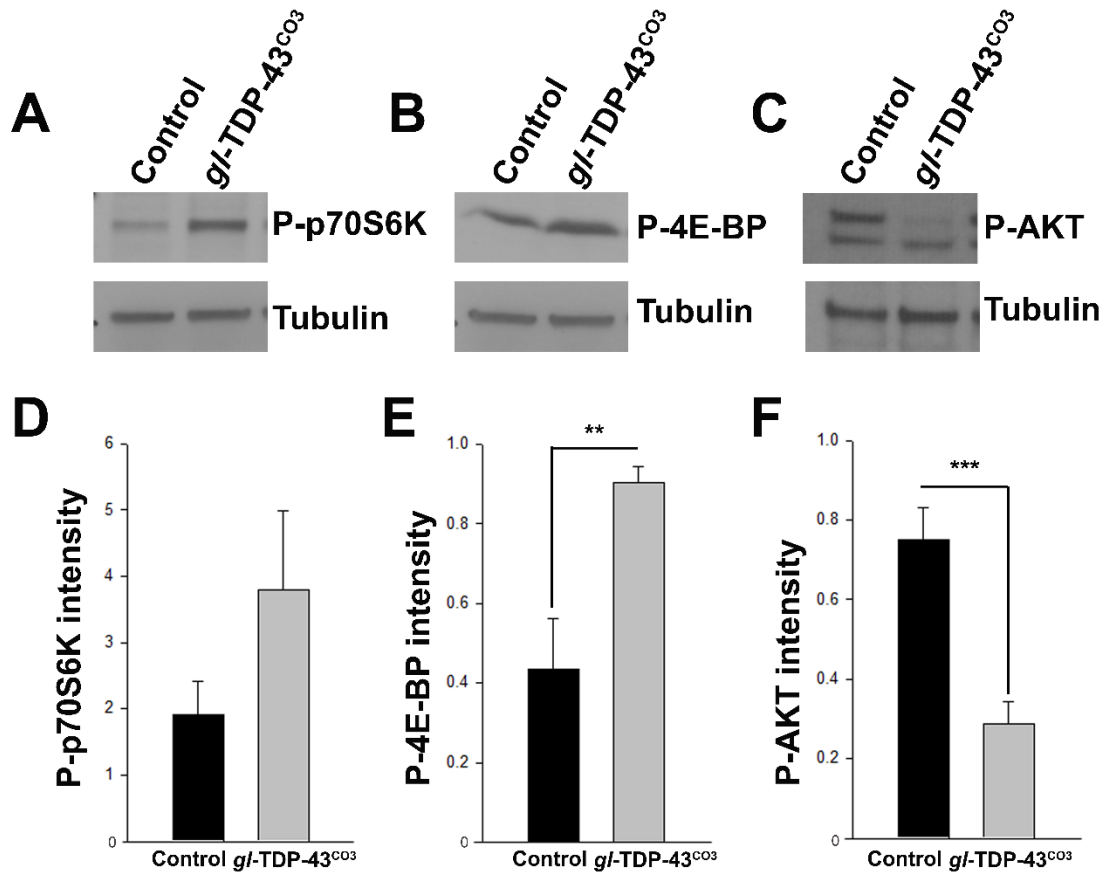


(A) represents a schematic of the adult eye and the area inside the rectangle is where the images were obtained. (B-E) Coexpression of codon optimized TDP-43 and autophagic protein Atg5-GFP shows that the large vacuoles present in 1 day post-eclosion adult retina is positive for Atg5 (scale bar 5 μ M). (F) represents the schematic of the third instar larval eye imaginal disc and the area in rectangle is the area imaged. (G-I) Another autophagic marker was coexpressed with codon optimized TDP-43, Atg8-mCherry-GFP, that is pH sensitive and only expresses GFP at a higher pH content. The TDP-43 expressed flies show that few of the relatively smaller punctae were positive for both Atg8 mCherry and

GFP (arrow heads), while majority of the punctae were only fluorescent for Atg8 mCherry (white arrows), indicating more acidic punctae (scale bar 10 μ M).

Genotypes: **(A-D)** w^{1118} , GMR-GAL4/ $w^{1118};g/-$ TDP-43^{CO3}/+;UAS-Atg5-GFP/+, **(E-G)** w^{1118} , GMR-GAL4/ $w^{1118};g/-$ TDP-43^{CO3}/UAS-Atg8-mCherry-GFP/+.

Figure 4.5. TDP-43 misexpression causes changes in the levels of proteins involved in the mTOR signaling pathway



Western blot analysis of codon optimized TDP-43 misexpression compared to wild type Canton S control for phospho-p70S6K protein **(A)** and phospho-4E-BP **(B)** show an increase in the protein level upon TDP-43 misexpression. The protein levels of phospho-AKT **(C)** show a decrease in one of the isomers of phospho-AKT upon TDP-43 misexpression. **(D-F)** represents the quantification of phospho-p70S6K, phospho-4E-BP and phospho-AKT blots, respectively. While there is no statistical significance between control and TDP-43 misexpressed flies, the phospho-p70S6K protein levels do show a visible increase. Phospho-

4E-BP protein levels show a statistically significant increase ($p < 0.02$) and the phospho-AKT protein levels show a statistically significant decrease ($p < 0.01$) in TDP-43 misexpressed flies. All statistical analysis was performed with paired Student's t-test with two-tailed distribution of equal variance.

CHAPTER V: SUMMARY AND FUTURE DIRECTIONS

5.1 Relevance of Codon Optimized Disease Model for TDP-43 Proteinopathies

Non-cell-autonomous toxicity in codon optimized TDP-43 transgenic model

There are many neurodegenerative disease models in the *Drosophila* that express human genes in the fly eye. Many of these proteins are known to affect different cell types in the eye. For example, in a polyglutamine-expanded human huntingtin transgenic model, the polyglutamine-expanded huntingtin has been shown to form nuclear inclusions and cause severe degeneration of photoreceptor cells (Jackson et al., 1998). Unlike this model, the human wild type tau transgenic model, shows abnormal polarity and some rhabdomere loss, but mostly affects the cone cells and ommatidial architecture (Jackson et al., 2002). Different neurodegenerative proteins exert different effects on the *Drosophila* eye. The codon optimized TDP-43 transgenic model not only shows a robust phenotype on the external eye, it also shows a robust phenotype on the internal structure and function of the eye. The external phenotype clearly affects different cell types in the fly retina, as evident by the depigmentation involving pigment cells, bristle irregularities involving interommatidial bristle cells and necrosis in the cone cells. TDP-43 might be interacting with the different types of cells to disrupt the normal morphology and function of these different cells to contribute to the external phenotype observed. These phenotypes indicate that TDP-43 is

affecting more than photoreceptor neurons and the pathology is most likely widespread among different cell types in the *Drosophila* retina.

Moreover, TDP-43 is known to be present and shows disease related pathology in different types of cells both in humans and in animal models (Mackenzie and Rademakers, 2008; Wegorzewska et al., 2009). In a *Drosophila* model, TDP-43 has been shown to exhibit individual responses in motor neurons and glial cells (Estes et al., 2013). It is possible that TDP-43 might also provoke cell type specific vulnerability in the *Drosophila* eye. Therefore, further investigation to evaluate the TDP-43 mediated effect on the different cells in the fly eye will lead us to a better understanding of cell type variability in TDP-43 mediated neurodegeneration. Based on the observed phenotype of the codon optimized TDP-43 flies, it is an ideal genetic tool to pursue such investigations that characterize the effect of TDP-43 misexpression in the eye by determining the morphological effect of TDP-43 in different cell types and by determining the localization of TDP-43 with respect to the different cell types.

Codon optimized TDP-43 transgenic model and genetic screens

As TDP-43 is a RNA-binding protein and its known functions involve RNA metabolism and regulation, there has been a lot of focus on identifying RNA targets of TDP-43. In order to characterize these targets, many have utilized cell cultures, mice models, and ALS and FTLN patient brain samples. Recently, TDP-43 was shown to bind approximately 30% of the mouse transcriptome, indicating

the vast amount of possible interactors that can associate with TDP-43 to regulate RNA processing and splicing (Polymenidou et al., 2011; Tollervey et al., 2011). Many of these putative modifiers bind the UG-rich sequence at introns of TDP-43 (Bhardwaj et al., 2013). Validating some of these putative modifiers of TDP-43 in an *in vivo* model, such as *Drosophila*, through biochemical and genetic manipulation can help us better understand the TDP-43 dependent disease mechanism in ALS and FTLD. The codon optimized TDP-43 model provides an ideal model to characterize and validate some of these modifiers in an *in vivo* system. The robust phenotypes observed in these flies can be scored easily for possible effectors of TDP-43 in a targeted genetic screen that will allow us to identify and pursue novel mechanisms for disease pathology.

In addition, forward genetic screens are also a great way to identify possible mechanisms of action. The development of fly retina and wing is regulated by a number of conserved pathways including Notch, BMP, and EGFR signaling (Adams et al., 2000). The external phenotypes seen using the codon optimized model could be interacting with substrates from these signaling pathway to induce those phenotypes. Using various genetic approaches, the exact mechanism underlying TDP-43 mediated phenotype in the eye or the wing can be analyzed. Such analysis may elucidate plausible targets of TDP-43 or RNA species regulated by TDP-43.

5.2 Autophagy and TDP-43

Presence of toxic TDP-43 aggregates have been well characterized in human patient samples of ALS and FTLN (Geser et al., 2009; Lee et al., 2010). While cell culture models and *in vitro* studies have shown TDP-43 forms toxic aggregates, not many wild-type TDP-43 animal models have shown robust production of TDP-43 aggregates (Couthouis et al., 2011; Guo et al., 2011; Lee et al., 2011). Previously, specific disease related mutations have been shown to be more toxic leading to an accumulation of these oligomeric species (Choksi et al., 2014; Guo et al., 2011; Johnson et al., 2009; Nonaka et al., 2009). The work presented here, shows a very similar accumulation of toxic aggregates, but in a wild type TDP-43 model. These protein aggregates are typically cleared by the cellular process known as autophagy that clears cytosolic components. A disruption in the autophagy process can lead to cellular imbalance and has been linked to many neurodegenerative diseases, including Alzheimer's disease, Parkinson's disease, Huntington's disease and ALS (Sasaki, 2011; Wong and Cuervo, 2010). In patients with sporadic ALS, accumulation of autophagosomes was observed in the spinal cord (Sasaki, 2011). In animal models, it has been evident that an inhibition of UPS or autophagy leads to increased TDP-43 aggregation and toxicity (Brady et al., 2011). In addition, p62 has been identified to directly bind with TDP-43 and an overexpression of p62 can reduce TDP-43 aggregation (Tanji et al., 2012).

In the codon optimized model, we observed an increase in acidic vacuoles that are positive for autophagic proteins involved in the formation of autophagosomes. We believe these acidic lysosomal vacuoles that we observe are mature autolysosomes that are induced in order to clear the cytoplasmic aggregates of TDP-43. To conclusively prove that autophagy is really at play, further characterization of these vacuoles is required. The use of electron microscopy to detect the characteristic double membrane structure of the autophagosomes, chemically inducing and inhibiting autophagy and genetic manipulation of key autophagic genes all remain a possibility for further investigation. Signaling pathways that regulate autophagy have yet to be investigated in a TDP-43 mediated neurodegenerative model. Most notably, the mTOR signaling pathway regulates the induction of autophagy upon cellular stress (Caccamo et al., 2009; Wang et al., 2012). While our initial studies using markers of mTOR signaling pathway were inconclusive, further investigation into the signaling pathways that regulate autophagy may provide us with valuable information. Involvement of autophagy in TDP-43 proteinopathies could unveil autophagy as a potential therapeutic target.

5.3 Concluding remarks

In summary, the purpose of the work presented here was to characterize a novel transgenic *Drosophila melanogaster* model of TDP-43 to study TDP-43 mediated neurodegeneration. The results presented here highlight the great potential for this model to be used to study various disease related mechanisms

using genetic manipulations. As very little is known about the exact mechanism of TDP-43 mediated neurodegeneration and the scarcity of treatment available for these neurodegenerative diseases, it is essential to identify how TDP-43 contributes to neurodegeneration and find possible therapeutic targets.

Bibliography

- Adams, M.D., Celniker, S.E., Holt, R.A., Evans, C.A., Gocayne, J.D., Amanatides, P.G., Scherer, S.E., Li, P.W., Hoskins, R.A., Galle, R.F., *et al.* (2000). The genome sequence of *Drosophila melanogaster*. *Science* 287, 2185-2195.
- Ambegaokar, S.S., and Jackson, G.R. (2011). Functional genomic screen and network analysis reveal novel modifiers of tauopathy dissociated from tau phosphorylation. *Hum Mol Genet* 20, 4947-4977.
- Arai, T., Mackenzie, I.R., Hasegawa, M., Nonaka, T., Niizato, K., Tsuchiya, K., Iritani, S., Onaya, M., and Akiyama, H. (2009). Phosphorylated TDP-43 in Alzheimer's disease and dementia with Lewy bodies. *Acta Neuropathol* 117, 125-136.
- Ash, P.E., Zhang, Y.J., Roberts, C.M., Saldi, T., Hutter, H., Buratti, E., Petrucelli, L., and Link, C.D. (2010). Neurotoxic effects of TDP-43 overexpression in *C. elegans*. *Hum Mol Genet* 19, 3206-3218.
- Ashford, T.P., and Porter, K.R. (1962). Cytoplasmic components in hepatic cell lysosomes. *J Cell Biol* 12, 198-202.
- Ayala, Y.M., Pantano, S., D'Ambrogio, A., Buratti, E., Brindisi, A., Marchetti, C., Romano, M., and Baralle, F.E. (2005). Human, *Drosophila*, and *C.elegans* TDP43: nucleic acid binding properties and splicing regulatory function. *J Mol Biol* 348, 575-588.

Bakhoun, M.F., Bakhoun, C.Y., Ding, Z., Carlton, S.M., Campbell, G.A., and Jackson, G.R. (2014). Evidence for autophagic gridlock in aging and neurodegeneration. *Transl Res* 3, 48-46.

Bellen, H.J., Levis, R.W., Liao, G., He, Y., Carlson, J.W., Tsang, G., Evans-Holm, M., Hiesinger, P.R., Schulze, K.L., Rubin, G.M., *et al.* (2004). The BDGP gene disruption project: single transposon insertions associated with 40% of *Drosophila* genes. *Genetics* 167, 761-781.

Bhardwaj, A., Myers, M.P., Buratti, E., and Baralle, F.E. (2013). Characterizing TDP-43 interaction with its RNA targets. *Nucleic Acids Res* 41, 5062-5074.

Bier, E. (2005). *Drosophila*, the golden bug, emerges as a tool for human genetics. *Nat Rev Genet* 6, 9-23.

Bilen, J., and Bonini, N.M. (2005). *Drosophila* as a model for human neurodegenerative disease. *Annu Rev Genet* 39, 153-171.

Bilen, J., and Bonini, N.M. (2007). Genome-wide screen for modifiers of ataxin-3 neurodegeneration in *Drosophila*. *PLoS Genet* 3, 1950-1964.

Brady, O.A., Meng, P., Zheng, Y., Mao, Y., and Hu, F. (2011). Regulation of TDP-43 aggregation by phosphorylation and p62/SQSTM1. *J Neurochem* 116, 248-259.

Brand, A.H., and Perrimon, N. (1993). Targeted gene expression as a means of altering cell fates and generating dominant phenotypes. *Development* 118, 401-415.

Bugiani, O. (2007). The many ways to frontotemporal degeneration and beyond. *Neurol Sci* 28, 241-244.

Buratti, E., Brindisi, A., Giombi, M., Tisminetzky, S., Ayala, Y.M., and Baralle, F.E. (2005). TDP-43 binds heterogeneous nuclear ribonucleoprotein A/B through its C-terminal tail: an important region for the inhibition of cystic fibrosis transmembrane conductance regulator exon 9 splicing. *J Biol Chem* 280, 37572-37584.

Caccamo, A., Majumder, S., Deng, J.J., Bai, Y., Thornton, F.B., and Oddo, S. (2009). Rapamycin rescues TDP-43 mislocalization and the associated low molecular mass neurofilament instability. *J Biol Chem* 284, 27416-27424.

Carthew, R.W. (2007). Pattern formation in the *Drosophila* eye. *Curr Opin Genet Dev* 17, 309-313.

Chatterjee, S., Sang, T.K., Lawless, G.M., and Jackson, G.R. (2009). Dissociation of tau toxicity and phosphorylation: role of GSK-3 β , MARK and Cdk5 in a *Drosophila* model. *Hum Mol Genet* 18, 164-177.

Chen-Plotkin, A.S., Lee, V.M., and Trojanowski, J.Q. (2010). TAR DNA-binding protein 43 in neurodegenerative disease. *Nat Rev Neurol* 6, 211-220.

Choksi, D.K., Roy, B., Chatterjee, S., Yusuff, T., Bakhoum, M.F., Sengupta, U., Ambegaokar, S., Kaye, R., and Jackson, G.R. (2014). TDP-43 Phosphorylation by casein kinase I ϵ promotes oligomerization and enhances toxicity in vivo. *Hum Mol Genet* 23, 1025-1035.

Clark, I.E., Dodson, M.W., Jiang, C., Cao, J.H., Huh, J.R., Seol, J.H., Yoo, S.J., Hay, B.A., and Guo, M. (2006) *Drosophila* pink1 is required for mitochondrial function and interacts genetically with parkin. *Nature* 441, 1162-1166.

Cohen, T.J., Lee, V.M., and Trojanowski, J.Q. (2011). TDP-43 functions and pathogenic mechanisms implicated in TDP-43 proteinopathies. *Trends Mol Med* 17, 659-667.

Couthouis, J., Hart, M.P., Shorter, J., DeJesus-Hernandez, M., Erion, R., Oristano, R., Liu, A.X., Ramos, D., Jethava, N., Hosangadi, D., *et al.* (2011). A yeast functional screen predicts new candidate ALS disease genes. *Proc Natl Acad Sci U S A* 108, 20881-20890.

Elden, A.C., Kim, H.J., Hart, M.P., Chen-Plotkin, A.S., Johnson, B.S., Fang, X., Armakola, M., Geser, F., Greene, R., Lu, M.M., *et al.* (2010). Ataxin-2 intermediate-length polyglutamine expansions are associated with increased risk for ALS. *Nature* 466, 1069-1075.

Estes, P.S., Boehringer, A., Zwick, R., Tang, J.E., Grigsby, B., and Zarnescu, D.C. (2011). Wild-type and A315T mutant TDP-43 exert differential neurotoxicity in a *Drosophila* model of ALS. *Hum Mol Genet* 20, 2308-2321.

Estes, P.S., Daniel, S.G., McCallum, A.P., Boehringer, A.V., Sukhina, A.S., Zwick, R.A., and Zarnescu, D.C. (2013). Motor neurons and glia exhibit specific individualized responses to TDP-43 expression in a *Drosophila* model of amyotrophic lateral sclerosis. *Dis Model Mech* 6, 721-733.

Fabian-Fine, R., Verstreken, P., Hiesinger, P.R., Horne, J.A., Kostyleva, R., Zhou, Y., Bellen, H.J., and Meinertzhagen, I.A. (2003). Endophilin promotes a late step in endocytosis at glial invaginations in *Drosophila* photoreceptor terminals. *J Neurosci* 23, 10732-10744.

Feany, M.B., and Bender, W.W. (2000). A *Drosophila* model of Parkinson's disease. *Nature* 404, 394-398.

Feigin, F., Godena, V.K., Romano, G., D'Ambrogio, A., Klima, R., and Baralle, F.E. (2009). Depletion of TDP-43 affects *Drosophila* motoneurons terminal synapsis and locomotive behavior. *FEBS Lett* 583, 1586-1592.

Fiesel, F.C., Voigt, A., Weber, S.S., Van den Haute, C., Waldenmaier, A., Gorner, K., Walter, M., Anderson, M.L., Kern, J.V., Rasse, T.M., *et al.* (2010). Knockdown of transactive response DNA-binding protein (TDP-43) downregulates histone deacetylase 6. *Embo J* 29, 209-221.

Filimonenko, M., Isakson, P., Finley, K.D., Anderson, M., Jeong, H., Melia, T.J., Bartlett, B.J., Myers, K.M., Birkeland, H.C., Lamark, T., *et al.* (2010). The selective macroautophagic degradation of aggregated proteins requires the PI3P-binding protein Alfy. *Mol Cell* 38, 265-279.

Filimonenko, M., Stuffers, S., Raiborg, C., Yamamoto, A., Malerod, L., Fisher, E.M., Isaacs, A., Brech, A., Stenmark, H., and Simonsen, A. (2007). Functional multivesicular bodies are required for autophagic clearance of protein aggregates associated with neurodegenerative disease. *J Cell Biol* 179, 485-500.

Finelli, A., Kelkar, A., Song, H.J., Yang, H., and Konsolaki, M. (2004). A model for studying Alzheimer's Abeta42-induced toxicity in *Drosophila melanogaster*. *Mol Cell Neurosci* 26, 365-375.

Finley, K.D., Edeen, P.T., Cumming, R.C., Mardahl-Dumesnil, M.D., Taylor, B.J., Rodriguez, M.H., Hwang, C.E., Benedetti, M., and McKeown, M. (2003). Blue

cheese mutations define a novel, conserved gene involved in progressive neural degeneration. *J Neurosci* 23, 1254-1264.

Freeman, M. (1996). Reiterative use of the EGF receptor triggers differentiation of all cell types in the *Drosophila* eye. *Cell* 87, 651-660.

Fulga, T.A., Elson-Schwab, I., Khurana, V., Steinhilb, M.L., Spires, T.L., Hyman, B.T., and Feany, M.B. (2007). Abnormal bundling and accumulation of F-actin mediates tau-induced neuronal degeneration in vivo. *Nat Cell Biol* 9, 139-148.

Gendron, T.F., Josephs, K.A., and Petrucelli, L. (2010). Review: transactive response DNA-binding protein 43 (TDP-43): mechanisms of neurodegeneration. *Neuropathol Appl Neurobiol* 36, 97-112.

Gendron, T.F., and Petrucelli, L. (2011). Rodent models of TDP-43 proteinopathy: investigating the mechanisms of TDP-43-mediated neurodegeneration. *J Mol Neurosci* 45, 486-499.

Geser, F., Martinez-Lage, M., Kwong, L.K., Lee, V.M., and Trojanowski, J.Q. (2009). Amyotrophic lateral sclerosis, frontotemporal dementia and beyond: the TDP-43 diseases. *J Neurol* 256, 1205-1214.

Godena, V.K., Romano, G., Romano, M., Appocher, C., Klima, R., Buratti, E., Baralle, F.E., and Feiguin, F. (2011). TDP-43 regulates *Drosophila* neuromuscular junctions growth by modulating Futsch/MAP1B levels and synaptic microtubules organization. *PLoS One* 6, e17808.

Gordon, P.H. (2013). Amyotrophic Lateral Sclerosis: An update for 2013 Clinical Features, Pathophysiology, Management and Therapeutic Trials. *Aging Dis* 4, 295-310.

Greene, J.C., Whitworth, A.J., Kuo, I., Andrews, L.A., Feany, M.B., and Pallanck, L.J. (2003). Mitochondrial pathology and apoptotic muscle degeneration in *Drosophila parkin* mutants. *Proc Natl Acad Sci U S A* 100, 4078-4083.

Guo, M., Hong, E.J., Fernandes, J., Zipursky, S.L., and Hay, B.A. (2003). A reporter for amyloid precursor protein gamma-secretase activity in *Drosophila*. *Hum Mol Genet* 12, 2669-2678.

Guo, W., Chen, Y., Zhou, X., Kar, A., Ray, P., Chen, X., Rao, E.J., Yang, M., Ye, H., Zhu, L., *et al.* (2011). An ALS-associated mutation affecting TDP-43 enhances protein aggregation, fibril formation and neurotoxicity. *Nat Struct Mol Biol* 18, 822-830.

Hanson, K.A., Kim, S.H., Wassarman, D.A., and Tibbetts, R.S. (2010). Ubiquitin modifies TDP-43 toxicity in a *Drosophila* model of amyotrophic lateral sclerosis (ALS). *J Biol Chem* 285, 11068-11072.

Hasegawa, M., Arai, T., Akiyama, H., Nonaka, T., Mori, H., Hashimoto, T., Yamazaki, M., and Oyanagi, K. (2007). TDP-43 is deposited in the Guam parkinsonism-dementia complex brains. *Brain* 130, 1386-1394.

Higashi, S., Iseki, E., Yamamoto, R., Minegishi, M., Hino, H., Fujisawa, K., Togo, T., Katsuse, O., Uchikado, H., Furukawa, Y., *et al.* (2007). Concurrence of TDP-43, tau and alpha-synuclein pathology in brains of Alzheimer's disease and dementia with Lewy bodies. *Brain Res* 12, 284-294.

Igaz, L.M., Kwong, L.K., Lee, E.B., Chen-Plotkin, A., Swanson, E., Unger, T., Malunda, J., Xu, Y., Winton, M.J., Trojanowski, J.Q., *et al.* (2011). Dysregulation

of the ALS-associated gene TDP-43 leads to neuronal death and degeneration in mice. *J Clin Invest* 121, 726-738.

Iijima, K., Liu, H.P., Chiang, A.S., Hearn, S.A., Konsolaki, M., and Zhong, Y. (2004). Dissecting the pathological effects of human Abeta40 and Abeta42 in *Drosophila*: a potential model for Alzheimer's disease. *Proc Natl Acad Sci U S A* 101, 6623-6628.

Jackson, G.R., Salecker, I., Dong, X., Yao, X., Arnheim, N., Faber, P.W., MacDonald, M.E., and Zipursky, S.L. (1998). Polyglutamine-expanded human huntingtin transgenes induce degeneration of *Drosophila* photoreceptor neurons. *Neuron* 21, 633-642.

Jackson, G.R., Wiedau-Pazos, M., Sang, T.K., Wagle, N., Brown, C.A., Massachi, S., and Geschwind, D.H. (2002). Human wild-type tau interacts with wiggless pathway components and produces neurofibrillary pathology in *Drosophila*. *Neuron* 34, 509-519.

Johnson, B.S., Snead, D., Lee, J.J., McCaffery, J.M., Shorter, J., and Gitler, A.D. (2009). TDP-43 is intrinsically aggregation-prone, and amyotrophic lateral sclerosis-linked mutations accelerate aggregation and increase toxicity. *J Biol Chem* 284, 20329-20339.

Karsten, S.L., Sang, T.K., Gehman, L.T., Chatterjee, S., Liu, J., Lawless, G.M., Sengupta, S., Berry, R.W., Pomakian, J., Oh, H.S., *et al.* (2006). A genomic screen for modifiers of tauopathy identifies puromycin-sensitive aminopeptidase as an inhibitor of tau-induced neurodegeneration. *Neuron* 51, 549-560.

Khurana, V., Lu, Y., Steinhilb, M.L., Oldham, S., Shulman, J.M., and Feany, M.B. (2006). TOR-mediated cell-cycle activation causes neurodegeneration in a *Drosophila* tauopathy model. *Curr Biol* 16, 230-241.

Kosmidis, S., Grammenoudi, S., Papanikolopoulou, K., and Skoulakis, E.M. (2010). Differential effects of Tau on the integrity and function of neurons essential for learning in *Drosophila*. *J Neurosci* 30, 464-477.

Kumar, J.P. (2001). Signalling pathways in *Drosophila* and vertebrate retinal development. *Nat Rev Genet* 2, 846-857.

Kumar, J.P. (2011). My what big eyes you have: how the *Drosophila* retina grows. *Dev Neurobiol* 71, 1133-1152.

Kundu, M., and Thompson, C.B. (2008). Autophagy: basic principles and relevance to disease. *Annu Rev Pathol* 3, 427-455.

Lamark, T., and Johansen, T. (2012). Aggrephagy: selective disposal of protein aggregates by macroautophagy. *Int J Cell Biol* 736905, 22.

Lanson, N.A., Jr., Maltare, A., King, H., Smith, R., Kim, J.H., Taylor, J.P., Lloyd, T.E., and Pandey, U.B. (2011). A *Drosophila* model of FUS-related neurodegeneration reveals genetic interaction between FUS and TDP-43. *Hum Mol Genet* 20, 2510-2523.

Lee, E.B., Lee, V.M., and Trojanowski, J.Q. (2011). Gains or losses: molecular mechanisms of TDP43-mediated neurodegeneration. *Nat Rev Neurosci* 13, 38-50.

Lee, J.H., Yu, W.H., Kumar, A., Lee, S., Mohan, P.S., Peterhoff, C.M., Wolfe, D.M., Martinez-Vicente, M., Massey, A.C., Sovak, G., *et al.* (2010). Lysosomal

proteolysis and autophagy require presenilin 1 and are disrupted by Alzheimer-related PS1 mutations. *Cell* 141, 1146-1158.

Li, H.Y., Yeh, P.A., Chiu, H.C., Tang, C.Y., and Tu, B.P. (2011). Hyperphosphorylation as a defense mechanism to reduce TDP-43 aggregation. *PLoS One* 6, e23075.

Li, Y., Ray, P., Rao, E.J., Shi, C., Guo, W., Chen, X., Woodruff, E.A., 3rd, Fushimi, K., and Wu, J.Y. (2010). A *Drosophila* model for TDP-43 proteinopathy. *Proc Natl Acad Sci U S A* 107, 3169-3174.

Li, Z., Lu, Y., Xu, X.L., and Gao, F.B. (2013). The FTD/ALS-associated RNA-binding protein TDP-43 regulates the robustness of neuronal specification through microRNA-9a in *Drosophila*. *Hum Mol Genet* 22, 218-225.

Liachko, N.F., Guthrie, C.R., and Kraemer, B.C. (2010). Phosphorylation promotes neurotoxicity in a *Caenorhabditis elegans* model of TDP-43 proteinopathy. *J Neurosci* 30, 16208-16219.

Lin, M.J., Cheng, C.W., and Shen, C.K. (2011). Neuronal function and dysfunction of *Drosophila* dTDP. *PLoS One* 6, e20371.

Lu, Y., Ferris, J., and Gao, F.B. (2009). Frontotemporal dementia and amyotrophic lateral sclerosis-associated disease protein TDP-43 promotes dendritic branching. *Mol Brain* 2, 30.

Mackenzie, I.R., and Rademakers, R. (2008). The role of transactive response DNA-binding protein-43 in amyotrophic lateral sclerosis and frontotemporal dementia. *Curr Opin Neurol* 21, 693-700.

Miguel, L., Frebourg, T., Campion, D., and Lecourtois, M. (2011). Both cytoplasmic and nuclear accumulations of the protein are neurotoxic in *Drosophila* models of TDP-43 proteinopathies. *Neurobiol Dis* 41, 398-406.

Mizushima, N. (2007). Autophagy: process and function. *Genes Dev* 21, 2861-2873.

Mizushima, N., and Levine, B. (2010). Autophagy in mammalian development and differentiation. *Nat Cell Biol* 12, 823-830.

Morimoto, N., Nagai, M., Ohta, Y., Miyazaki, K., Kurata, T., Morimoto, M., Murakami, T., Takehisa, Y., Ikeda, Y., Kamiya, T., *et al.* (2007). Increased autophagy in transgenic mice with a G93A mutant SOD1 gene. *Brain Res* 5, 112-117.

Muqit, M.M., and Feany, M.B. (2002). Modelling neurodegenerative diseases in *Drosophila*: a fruitful approach? *Nat Rev Neurosci* 3, 237-243.

Nair, U., and Klionsky, D.J. (2005). Molecular mechanisms and regulation of specific and nonspecific autophagy pathways in yeast. *J Biol Chem* 280, 41785-41788.

Neufeld, T.P. (2010). TOR-dependent control of autophagy: biting the hand that feeds. *Curr Opin Cell Biol* 22, 157-168.

Neumann, M., Sampathu, D.M., Kwong, L.K., Truax, A.C., Micsenyi, M.C., Chou, T.T., Bruce, J., Schuck, T., Grossman, M., Clark, C.M., *et al.* (2006). Ubiquitinated TDP-43 in frontotemporal lobar degeneration and amyotrophic lateral sclerosis. *Science* 314, 130-133.

Nonaka, T., Kametani, F., Arai, T., Akiyama, H., and Hasegawa, M. (2009). Truncation and pathogenic mutations facilitate the formation of intracellular aggregates of TDP-43. *Hum Mol Genet* 18, 3353-3364.

Ou, S.H., Wu, F., Harrich, D., Garcia-Martinez, L.F., and Gaynor, R.B. (1995). Cloning and characterization of a novel cellular protein, TDP-43, that binds to human immunodeficiency virus type 1 TAR DNA sequence motifs. *J Virol* 69, 3584-3596.

Pan, X.D., and Chen, X.C. (2013). Clinic, neuropathology and molecular genetics of frontotemporal dementia: a mini-review. *Transl Neurodegener* 2, 2047-9158.

Pandey, U.B., Nie, Z., Batlevi, Y., McCray, B.A., Ritson, G.P., Nedelsky, N.B., Schwartz, S.L., DiProspero, N.A., Knight, M.A., Schuldiner, O., *et al.* (2007). HDAC6 rescues neurodegeneration and provides an essential link between autophagy and the UPS. *Nature* 447, 859-863.

Pankiv, S., Clausen, T.H., Lamark, T., Brech, A., Bruun, J.A., Outzen, H., Overvatn, A., Bjorkoy, G., and Johansen, T. (2007). p62/SQSTM1 binds directly to Atg8/LC3 to facilitate degradation of ubiquitinated protein aggregates by autophagy. *J Biol Chem* 282, 24131-24145.

Park, J.H., Schroeder, A.J., Helfrich-Forster, C., Jackson, F.R., and Ewer, J. (2003). Targeted ablation of CCAP neuropeptide-containing neurons of *Drosophila* causes specific defects in execution and circadian timing of ecdysis behavior. *Development* 130, 2645-2656.

Polymenidou, M., Lagier-Tourenne, C., Hutt, K.R., Huelga, S.C., Moran, J., Liang, T.Y., Ling, S.C., Sun, E., Wancewicz, E., Mazur, C., *et al.* (2011). Long

pre-mRNA depletion and RNA missplicing contribute to neuronal vulnerability from loss of TDP-43. *Nat Neurosci* 14, 459-468.

Pressman, P.S., and Miller, B.L. (2013). Diagnosis and Management of Behavioral Variant Frontotemporal Dementia. *Biol Psychiatry* 13, 987-986.

Ratnaparkhi, A., Lawless, G.M., Schweizer, F.E., Golshani, P., and Jackson, G.R. (2008). A *Drosophila* model of ALS: human ALS-associated mutation in VAP33A suggests a dominant negative mechanism. *PLoS One* 3, e2334.

Ravikumar, B., Sarkar, S., Davies, J.E., Futter, M., Garcia-Arencibia, M., Green-Thompson, Z.W., Jimenez-Sanchez, M., Korolchuk, V.I., Lichtenberg, M., Luo, S., *et al.* (2010). Regulation of mammalian autophagy in physiology and pathophysiology. *Physiol Rev* 90, 1383-1435.

Riedl, L., Mackenzie, I.R., Forstl, H., Kurz, A., and Diehl-Schmid, J. (2014) Frontotemporal lobar degeneration: current perspectives. *Neuropsychiatr Dis Treat.* 10, 297-310.

Ritson, G.P., Custer, S.K., Freibaum, B.D., Guinto, J.B., Geffel, D., Moore, J., Tang, W., Winton, M.J., Neumann, M., Trojanowski, J.Q., *et al.* (2010). TDP-43 mediates degeneration in a novel *Drosophila* model of disease caused by mutations in VCP/p97. *J Neurosci* 30, 7729-7739.

Romano, M., Feiguin, F., and Buratti, E. (2012). *Drosophila* Answers to TDP-43 Proteinopathies. *J Amino Acids* 2012, 356081.

Rubinsztein, D.C. (2006). The roles of intracellular protein-degradation pathways in neurodegeneration. *Nature* 443, 780-786.

- Sabatelli, M., Conte, A., and Zollino, M. (2013). Clinical and genetic heterogeneity of amyotrophic lateral sclerosis. *Clin Genet* 83, 408-416.
- Salado, I.G., Redondo, M., Bello, M.L., Perez, C., Liachko, N.F., Kraemer, B.C., Miguel, L., Lecourtois, M., Gil, C., Martinez, A., *et al.* (2014). Protein kinase CK-1 inhibitors as new potential drugs for Amyotrophic Lateral Sclerosis. *J Med Chem* 57, 2755-2772.
- Sang, T.K., Chang, H.Y., Lawless, G.M., Ratnaparkhi, A., Mee, L., Ackerson, L.C., Maidment, N.T., Krantz, D.E., and Jackson, G.R. (2007). A *Drosophila* model of mutant human parkin-induced toxicity demonstrates selective loss of dopaminergic neurons and dependence on cellular dopamine. *J Neurosci* 27, 981-992.
- Sang, T.K., and Jackson, G.R. (2005). *Drosophila* models of neurodegenerative disease. *NeuroRx* 2, 438-446.
- Sang, T.K., Li, C., Liu, W., Rodriguez, A., Abrams, J.M., Zipursky, S.L., and Jackson, G.R. (2005). Inactivation of *Drosophila* Apaf-1 related killer suppresses formation of polyglutamine aggregates and blocks polyglutamine pathogenesis. *Hum Mol Genet* 14, 357-372.
- Sasaki, S. (2011). Autophagy in spinal cord motor neurons in sporadic amyotrophic lateral sclerosis. *J Neuropathol Exp Neurol* 70, 349-359.
- Schmid, B., Hruscha, A., Hogg, S., Banzhaf-Strathmann, J., Strecker, K., van der Zee, J., Teucke, M., Eimer, S., Hegemann, J., Kittelmann, M., *et al.* (2013). Loss of ALS-associated TDP-43 in zebrafish causes muscle degeneration, vascular

dysfunction, and reduced motor neuron axon outgrowth. *Proc Natl Acad Sci U S A* 110, 4986-4991.

Scott, R.C., Juhasz, G., and Neufeld, T.P. (2007). Direct induction of autophagy by Atg1 inhibits cell growth and induces apoptotic cell death. *Curr Biol* 17, 1-11.

Scott, R.C., Schuldiner, O., and Neufeld, T.P. (2004). Role and regulation of starvation-induced autophagy in the *Drosophila* fat body. *Dev Cell* 7, 167-178.

Scotter, E.L., Vance, C., Nishimura, A.L., Lee, Y.B., Chen, H.J., Urwin, H., Sardone, V., Mitchell, J.C., Rogelj, B., Rubinsztein, D.C., *et al.* (2014). Differential roles of the ubiquitin proteasome system (UPS) and autophagy in the clearance of soluble and aggregated TDP-43 species. *J Cell Sci* 127, 1263-1278.

Shulman, J.M., and Feany, M.B. (2003). Genetic modifiers of tauopathy in *Drosophila*. *Genetics* 165, 1233-1242.

Stallings, N.R., Puttaparthi, K., Luther, C.M., Burns, D.K., and Elliott, J.L. (2010). Progressive motor weakness in transgenic mice expressing human TDP-43. *Neurobiol Dis* 40, 404-414.

Steinhilb, M.L., Dias-Santagata, D., Fulga, T.A., Felch, D.L., and Feany, M.B. (2007a). Tau phosphorylation sites work in concert to promote neurotoxicity in vivo. *Mol Biol Cell* 18, 5060-5068.

Steinhilb, M.L., Dias-Santagata, D., Mulkearns, E.E., Shulman, J.M., Biernat, J., Mandelkow, E.M., and Feany, M.B. (2007b). S/P and T/P phosphorylation is critical for tau neurotoxicity in *Drosophila*. *J Neurosci Res* 85, 1271-1278.

- Tang, C.Y., and Sun, Y.H. (2002). Use of mini-white as a reporter gene to screen for GAL4 insertions with spatially restricted expression pattern in the developing eye in drosophila. *Genesis* 34, 39-45.
- Tanji, K., Zhang, H.X., Mori, F., Kakita, A., Takahashi, H., and Wakabayashi, K. (2012). p62/sequestosome 1 binds to TDP-43 in brains with frontotemporal lobar degeneration with TDP-43 inclusions. *J Neurosci Res* 90, 2034-2042.
- Tashiro, Y., Urushitani, M., Inoue, H., Koike, M., Uchiyama, Y., Komatsu, M., Tanaka, K., Yamazaki, M., Abe, M., Misawa, H., *et al.* (2012). Motor neuron-specific disruption of proteasomes, but not autophagy, replicates amyotrophic lateral sclerosis. *J Biol Chem* 287, 42984-42994.
- Temiz, P., Weihl, C.C., and Pestronk, A. (2009). Inflammatory myopathies with mitochondrial pathology and protein aggregates. *J Neurol Sci* 278, 25-29.
- Therrien, M., Wong, A.M., Kwan, E., and Rubin, G.M. (1999). Functional analysis of CNK in RAS signaling. *Proc Natl Acad Sci U S A* 96, 13259-13263.
- Tollervey, J.R., Curk, T., Rogelj, B., Briese, M., Cereda, M., Kayikci, M., Konig, J., Hortobagyi, T., Nishimura, A.L., Zupunski, V., *et al.* (2011). Characterizing the RNA targets and position-dependent splicing regulation by TDP-43. *Nat Neurosci* 14, 452-458.
- Tsachaki, M., and Sprecher, S.G. (2012). Genetic and developmental mechanisms underlying the formation of the Drosophila compound eye. *Dev Dyn* 241, 40-56.
- Tsai, K.J., Yang, C.H., Fang, Y.H., Cho, K.H., Chien, W.L., Wang, W.T., Wu, T.W., Lin, C.P., Fu, W.M., and Shen, C.K. (2010). Elevated expression of TDP-

43 in the forebrain of mice is sufficient to cause neurological and pathological phenotypes mimicking FTL-D. *J Exp Med* 207, 1661-1673.

Turner, M.R., Bowser, R., Bruijn, L., Dupuis, L., Ludolph, A., McGrath, M., Manfredi, G., Maragakis, N., Miller, R.G., Pullman, S.L., *et al.* (2013). Mechanisms, models and biomarkers in amyotrophic lateral sclerosis. *Amyotroph Lateral Scler Frontotemporal Degener* 1, 19-32.

Vaccaro, A., Tauffenberger, A., Aggad, D., Rouleau, G., Drapeau, P., and Parker, J.A. (2012). Mutant TDP-43 and FUS cause age-dependent paralysis and neurodegeneration in *C. elegans*. *PLoS One* 7, e31321.

Vanden Broeck, L., Naval-Sanchez, M., Adachi, Y., Diaper, D., Dourlen, P., Chapuis, J., Kleinberger, G., Gistelink, M., Van Broeckhoven, C., Lambert, J.C., *et al.* (2013). TDP-43 loss-of-function causes neuronal loss due to defective steroid receptor-mediated gene program switching in *Drosophila*. *Cell Rep* 3, 160-172.

Wang, I.F., Guo, B.S., Liu, Y.C., Wu, C.C., Yang, C.H., Tsai, K.J., and Shen, C.K. (2012). Autophagy activators rescue and alleviate pathogenesis of a mouse model with proteinopathies of the TAR DNA-binding protein 43. *Proc Natl Acad Sci U S A* 109, 15024-15029.

Wang, J.W., Brent, J.R., Tomlinson, A., Shneider, N.A., and McCabe, B.D. (2011). The ALS-associated proteins FUS and TDP-43 function together to affect *Drosophila* locomotion and life span. *J Clin Invest* 121, 4118-4126.

- Wang, X., Fan, H., Ying, Z., Li, B., Wang, H., and Wang, G. (2010). Degradation of TDP-43 and its pathogenic form by autophagy and the ubiquitin-proteasome system. *Neurosci Lett* 469, 112-116.
- Warrick, J.M., Chan, H.Y., Gray-Board, G.L., Chai, Y., Paulson, H.L., and Bonini, N.M. (1999). Suppression of polyglutamine-mediated neurodegeneration in *Drosophila* by the molecular chaperone HSP70. *Nat Genet* 23, 425-428.
- Warrick, J.M., Paulson, H.L., Gray-Board, G.L., Bui, Q.T., Fischbeck, K.H., Pittman, R.N., and Bonini, N.M. (1998). Expanded polyglutamine protein forms nuclear inclusions and causes neural degeneration in *Drosophila*. *Cell* 93, 939-949.
- Watson, M.R., Lagow, R.D., Xu, K., Zhang, B., and Bonini, N.M. (2008). A *drosophila* model for amyotrophic lateral sclerosis reveals motor neuron damage by human SOD1. *J Biol Chem* 283, 24972-24981.
- Wegorzewska, I., Bell, S., Cairns, N.J., Miller, T.M., and Baloh, R.H. (2009). TDP-43 mutant transgenic mice develop features of ALS and frontotemporal lobar degeneration. *Proc Natl Acad Sci U S A* 106, 18809-18814.
- Williamson, W.R., Wang, D., Haberman, A.S., and Hiesinger, P.R. (2010). A dual function of V0-ATPase a1 provides an endolysosomal degradation mechanism in *Drosophila melanogaster* photoreceptors. *J Cell Biol* 189, 885-899.
- Wils, H., Kleinberger, G., Janssens, J., Pereson, S., Joris, G., Cuijt, I., Smits, V., Ceuterick-de Groote, C., Van Broeckhoven, C., and Kumar-Singh, S. (2010). TDP-43 transgenic mice develop spastic paralysis and neuronal inclusions

characteristic of ALS and frontotemporal lobar degeneration. *Proc Natl Acad Sci U S A* 107, 3858-3863.

Wong, E., and Cuervo, A.M. (2010). Autophagy gone awry in neurodegenerative diseases. *Nat Neurosci* 13, 805-811.

Xu, Y.F., Gendron, T.F., Zhang, Y.J., Lin, W.L., D'Alton, S., Sheng, H., Casey, M.C., Tong, J., Knight, J., Yu, X., *et al.* (2010). Wild-type human TDP-43 expression causes TDP-43 phosphorylation, mitochondrial aggregation, motor deficits, and early mortality in transgenic mice. *J Neurosci* 30, 10851-10859.

Yang, Z., and Klionsky, D.J. (2010). Eaten alive: a history of macroautophagy. *Nat Cell Biol* 12, 814-822.

Zhang, T., Hwang, H.Y., Hao, H., Talbot, C., Jr., and Wang, J. (2012). *Caenorhabditis elegans* RNA-processing protein TDP-1 regulates protein homeostasis and life span. *J Biol Chem* 287, 8371-8382.

Vita

Tanzeen Yusuff was born on September 6th, 1986 in Chittagong, Bangladesh. She is the youngest child of Jamal Yusuff and Roshan Jahan. After moving to Texas in 2001, she has attended Lawrance D. Bell High School in Hurst, Texas and graduated in 2004. She then attended University of Texas at Austin, where she studied neurobiology and worked as an undergraduate research assistant in Dr. Nigel S. Atkinson's laboratory. She graduated with a Bachelor of Science degree in 2008. She entered the Graduate School of Biomedical Sciences at the University of Texas Medical Branch in 2009. Soon after, she joined the laboratory of Dr. George R. Jackson and the Neuroscience Graduate Program. During her graduate career, she has published one research article in collaboration with her fellow lab members and has taught as part of the undergraduate toxicology course at the Texas A&M University Galveston.

Permanent address: 160 East Plaza Boulevard, Apt# 2177, Hurst, TX 76053

This dissertation was typed by Tanzeen Yusuff.